BASIC HELIX LOOP HELIX ENHANCER 40 IN NEURONAL EXCITABILITY AND SYNAPTIC PLASTICITY

by

Kelly Andrew Hamilton

A Dissertation
Submitted to the
Graduate Faculty
of
George Mason University
in Partial Fulfillment of
The Requirements for the Degree
of
Doctor of Philosophy
Neuroscience

Committee:

	Dr. Robert H. Lipsky, Dissertation Director
	Dr. Mark P. Mattson, Committee Member
	Dr. Ann Marini, Committee Member
	Dr. Daniel N. Cox, Committee Member
	Dr. Nadine Kabbani, Committee Member
	Dr. Saleet Jafri, Interim Director, Krasnow Institute for Advanced Studies
	Dr. Donna M. Fox, Associate Dean, Office of Student Affairs & Special Programs, College of Science
	Dr. Peggy Agouris, Dean, College of Science
Date: 8/23/16	Fall Semester 2016 George Mason University Fairfax, VA

Basic Helix Loop Helix Enhancer 40 in Neuronal Excitability and Synaptic Plasticity

A Dissertation submitted in partial fulfillment of the requirements for the degree of Doctor of Philosophy at George Mason University

by

Kelly Andrew Hamilton
Bachelor of Science
George Mason University, 2008

Director: Robert H. Lipsky, Professor
Department of Neuroscience

Fall Semester 2016
George Mason University
Fairfax, VA

DEDICATION

In loving memory of Donna Annette Hamilton, my mother and motivation.

ACKNOWLEDGEMENTS

I would like to thank Robert Lipsky and Mark Mattson for taking me in through a difficult lab transition and providing me with the lab space, resources, and mentorship to see this project through. Thanks also to committee members Ann Marini, Nadine Kabbani, and Dan Cox who stayed with on as a mentor despite relocating his laboratory to another university. Further, I'd like to thank the George Mason University Provost office for providing me with a dissertation completion grant for the spring 2016 semester and to Saleet Jafri, the acting department chair, who helped with funding. And I'd like to give special thanks to several lab members at the Laboratory of Neurosciences at the National Institute on Aging who played critical roles in moving this project forward: Yue Wang who mentored me in electrophysiology and performed multiple essential experiments for this project; experimental help from: Sophia Raefsky, Sean Berkowitz, Ryan Spangler, and Caitlin Suire; Ruiqian Wan who trained me to do *in vivo* work with mice; Emmette Hutchinson who trained me in various techniques and gave lots of constructive feedback; Mark Wilson who has been a very helpful lab manager; Karen Harris for dealing with my numerous appointments and administrative work; and Simonetta Camandola for providing guidance and invaluable feedback on experimental design and troubleshooting.

TABLE OF CONTENTS

LIST OF TABLES

LIST OF FIGURES

LIST OF ABBREVIATIONS

Amyloid Beta	Aβ
Artificial cerebral spinal fluid	ACSF
Brain derived neurotrophic factor	BDNF
Basic helix loop helix	bHLH
Basic helix loop helix enhancer 40	Bhlhe40
Congenic *Bhlhe40* knock out mouse	*Bhlhe40* KO
Mixed background *Bhlhe40* knock out mouse	*Bhlhe40* KO-mix
Basic helix loop helix enhancer 41	Bhlhe41
Calmodulin kinase 1d	Camk1d
Carbohydrate response element	ChoRE
Carbohydrate response element binding protein	ChREBP
Cerebellum	CER
Cortex	CTX
Cyclic AMP response element binding protein	CREB
Electroencephalogram	EEG
Embryonic day	E
Enzyme-linked immunosorbent assay	ELISA
Excitatory postsynaptic current	EPSC
Excitatory postsynaptic potential	EPSP
False discovery rate	FDR
$GABA_B$ receptor subunit 1 gene	*Gabbr1*
$GABA_B$ receptor subunit 1 protein	$GABA_BR1$
GABA receptor associated protein	*Gabarap*
$GABA_A$ receptor subunit gamma 2	Gabrg2
Gamma-aminobutyric acid	GABA
Glutamate receptor subunit 1 gene	*Gria1*
Glutamate receptor subunit 1 protein	GluR1
Glutamate receptor subunit 2 protein	GluR2
High frequency stimulation	HFS
Hippocampus	HIPP
Insulin degrading enzyme	Ide
Insulin growth factor 1	Igf1
Insulin growth factor 2	Igf2
Input/Output	I/O
Intraperitoneally	IP
Inhibitory Postsynaptic Current	IPSC

Kainic acid ..... KA
Knock out ..... KO
Low frequency stimulation ..... LFS
Long term depression ..... LTD
Long term potentiation ..... LTP
Miniature excitatory postsynaptic current ..... mEPSC
Macrophage inhibitory cytokine-1 ..... MIC-1
Morris water maze ..... MWM
N-methyl-D-aspartate Receptor ..... NMDAR
Neurotrophic receptor tyrosine kinase 3 gene *NTrk3*
Paired-pulse facilitation ..... PPF
Parameterized analysis of gene enrichment ..... PAGE
Period1 ..... Per1
Postnatal day ..... P
Principal component analysis ..... PCA
Quantitative reverse-transcription polymerase chain reaction ..... qRT-PCR
Schaffer collateral ..... SC
Wild type ..... WT

ABSTRACT

BASIC HELIX LOOP HELIX ENHANCER 40 IN NEURONAL EXCITABILITY AND SYNAPTIC PLASTICITY

Kelly Andrew Hamilton, PhD

George Mason University, 2016

Dissertation Director: Dr. Robert H. Lipsky

This dissertation describes the role of the Basic helix loop helix enhancer 40 (Bhlhe40) transcription factor in the adult murine brain at the molecular, cellular, network, and behavioral levels. Studies for this dissertation were performed on a congenic *Bhlhe40* gene knock out mouse model (*Bhlhe40* KO). The inspiration for this research project was based on prior findings in mice that were genetically null for the *Bhlhe40* gene on a mixed genetic background (Jiang et al., 2008, *J. Neurosci*). Mixed background *Bhlhe40* KO mice had enhanced seizure activity when injected intraperitoneally with the convulsant, kainic acid (KA). In the hippocampus, brain derived neurotrophic factor (BDNF) expression is increased following seizure activity and is thought to lower the threshold for subsequent seizures, implicating BDNF in a positive feedback loop in epileptogenesis. Specifically, mixed background *Bhlhe40* KO mice had elevated basal levels of *Bdnf-4* transcripts, which are normally expressed in an

activity-dependent manner. The central hypothesis of this research was that congenic *Bhlhe40* KO mice would have enhanced responses to KA-induced seizures due to excessive levels of basal BDNF. It was further thought that there would be coincident increases in neuronal activity in hippocampal slices and increased expression of genes modulating neuronal excitability.

The first objective of this research was to elucidate changes in gene expression occurring in the hippocampus of congenic *Bhlhe40* KO mice. A whole genome expression array was utilized to capture an unbiased profile of hippocampal mRNA levels from *Bhlhe40* KO mice compared to wild type (WT) mice. Gene expression array findings were independently validated by quantitative gene specific mRNA and protein assays. I found that insulin degrading enzyme (IDE) mRNA and protein levels were two-fold decreased in congenic *Bhlhe40* KO hippocampi. Unlike in the mixed background *Bhlhe40* KO mice, congenic *Bhlhe40* KO hippocampi did not have elevated levels of *Bdnf* mRNA or protein.

At the cellular level, I sought to determine the role of *Bhlhe40* KO in neuronal excitability. To test this, *Bhlhe40* KO hippocampal CA1 neurons, cells that express *Bhlhe40* in WT mice, were measured for excitatory and inhibitory electrophysiological properties and were determined to have enhanced excitation and reduced inhibition, indicating a hyperexcitable state. At the network level, electrophysiological field recordings from CA1 neurons in *Bhlhe40* KO and WT hippocampal slices revealed a decrease in both long term potentiation (LTP) and long term depression (LTD), indicating an overall reduction in long term synaptic plasticity.

At the behavioral level, I tested seizure severity in *Bhlhe40* KO mice by intra-hippocampal KA-injection but, despite the increase in excitability on the cellular level, I found no significant difference in seizure response between *Bhlhe40* KO mice and WT controls. In addition, exploratory behavior and learning and memory performance was determined in untreated congenic *Bhlhe40* KO and WT mice. Despite the reduction in synaptic plasticity, no changes in spatial learning and memory were observed on the Morris water maze; however, there was a decrease in exploratory behavior in the open field test, which may indicate increased anxiety.

An interesting finding from this work was the effect of genetic background, namely in regards to seizure susceptibility and *Bdnf* expression. Inter-strain differences can be explained at the genomic level by variation in promoter and other regulatory sequences in the genome. Importantly, I propose here that changes in IDE protein levels may be driving changes in basal excitability and reduced synaptic responses to stimulation, as well as a possible anxiety phenotype in *Bhlhe40* KO mice. Insulin levels were investigated and found to be not significantly changed in *Bhlhe40* KO hippocampus, however, IDE also degrades insulin-like growth factors -1 and -2, and amyloid beta. Further investigation into these other IDE substrates may elucidate the link between Bhlhe40-mediated IDE regulation, anxiety, neuronal excitability and synaptic plasticity.

CHAPTER ONE: BASIC HELIX LOOP HELIX ENHANCER 40 AND THE CENTRAL NERVOUS SYSTEM

Wrote Chapter: Kelly Hamilton
Edited Chapter: Robert Lipsky

Basic Helix Loop Helix Enhancer 40: Transcriptional Roles and Gene Expression

Basic helix loop helix enhancer 40 (Bhlhe40; also known as Clast5, Stra13, Sharp2, Dec1, Eip1, CR-8, and Bhlhb2) is a basic helix loop helix (bHLH) transcription factor that represses gene activity directly by binding to class B E-box sequences (CACGTG) with high affinity as a homodimer (St-Pierre et al., 2002; Kato et al., 2014). Bhlhe40 homodimers also binds to CATGTG and CACGTN (N=any nucleotide) and with low affinity to CACGCG (Yamada and Miyamoto, 2005), as well as to CTCGTG (Jiang et al., 2008). When bound to E boxes, Bhlhe40 homodimers repress transcriptional activity by interacting with transcriptional machinery (TBP and TFIIB) or by interacting with corepressors (HDAC1, NCoR, and mSin3A) at its C-terminal (Yamada and Miyamoto, 2005; Figure 1).

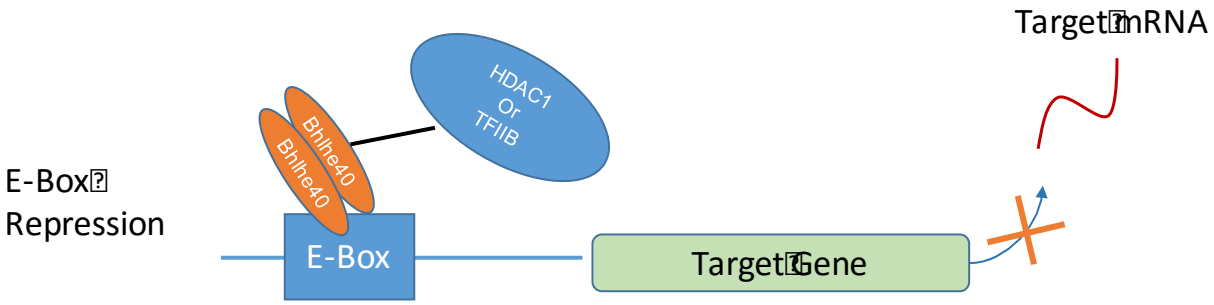

Figure 1. Canonical Bhlhe40-mediated gene repression via E-box binding.
The strongest known binding affinity of Bhlhe40 is for Class B E-boxes (CACGTG).

The helix-loop-helix domain of Bhlhe40 is responsible for dimerization and the basic domain is responsible for DNA binding. Bhlhe41 is the sister protein to Bhlhe40 and shares identical sequence identity in the basic and helix loop helix domains (Sun et al., 2007a). Therefore, Bhlhe40 can function as a homodimer or as a heterodimer with Bhlhe41 and bind to the same E-box targets (Kato et al., 2014). Bhlhe40 and Bhlhe41 share only 47% overall amino acid sequence identity, however, due to differences in the C-terminus, namely a large proline rich domain in Bhlhe40 and a large alanine/glycine rich domain in Bhlhe41 (Ow et al., 2014). This difference in the C-terminus is noteworthy because it is likely responsible for differential protein interactions between Bhlhe40 and Bhlhe41; for example, the recruitment of the histone methyltransferase G9a by Bhlhe41, but not Bhlhe40 (Ow et al., 2014).

In addition to its canonical roles described above, Bhlhe40 can activate (Li et al., 2006) and inhibit (Hsiao et al., 2009; Qian et al., 2012a) gene expression by interacting with other transcription factors. E-box bound Bhlhe40 can form a complex with MyoD, an E-box-binding bHLH transcriptional activator, when MyoD and Bhlhe40 E-boxes are

in close proximity, thereby repressing MyoD-mediated activation (Hsiao et al., 2009, Hsiao and Chen, 2010). E-box bound Bhlhe40 was also found to interact with p53 and prevent p53-mediated upregulation of macrophage inhibitory cytokine-1, thereby indirectly inducing apoptosis (Qian et al., 2012a). Bhlhe40, however, does not repress p53 activity at all p53 targets, and it is thought that this Bhlhe40-mediated repression only occurs where Bhlhe40 and p53 promoter elements are in close proximity (Qian et al., 2012a; Qian et al., 2012b). Interestingly, in addition to its role as a repressor, Bhlhe40 was found to bind to Sp1 sites and upregulate gene expression as part of the Sp1-DNA complex (Li et al., 2006; Qian et al., 2011). Together this indicates that 1) Bhlhe40 represses gene expression in the DNA-bound state by interacting with other transcription factors, in addition to its previously known interactions with basal transcriptional machinery and co-repressors; 2) that the spacing of regulatory elements (E-box elements) likely plays a role in regulating Bhlhe40-mediated transcriptional activity; and 3) Bhlhe40 is likely part of the Sp1 transcriptional activation machinery (Figure 2).

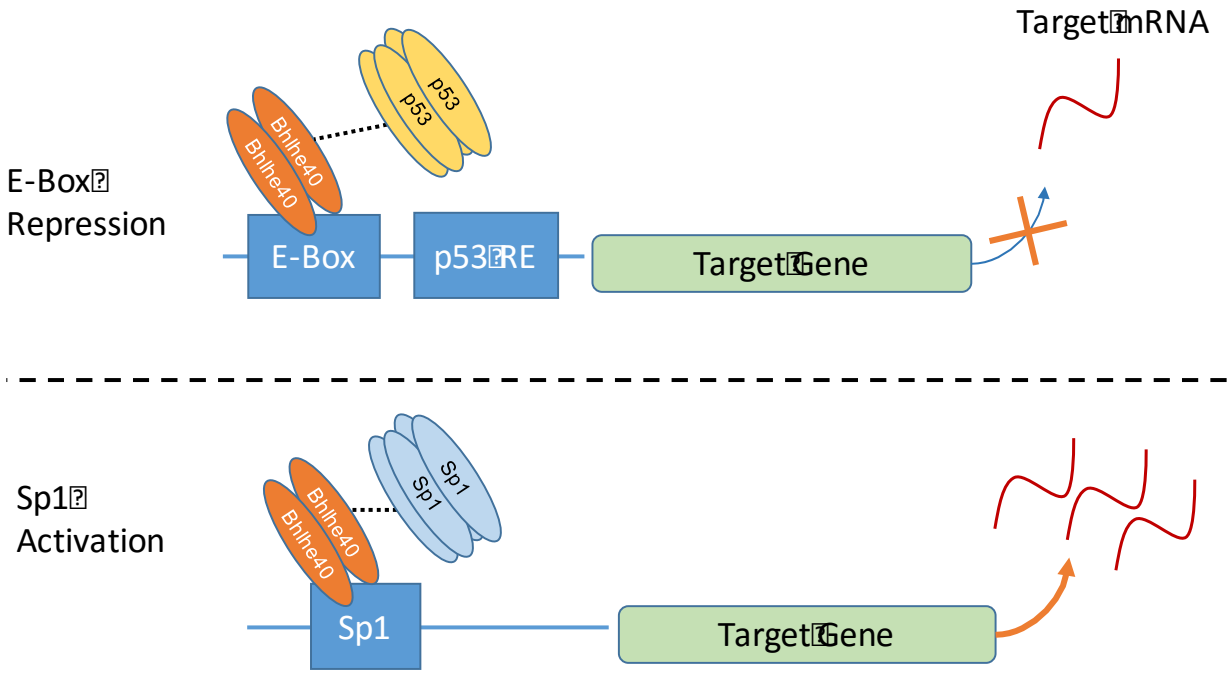

Figure 2. Non-canonical Bhlhe40-mediated transcriptional repression and activation.

Bhlhe40 gene expression starts at embryonic day (E) 8.5 in decidual tissue and trophoblast giant cells around the yolk sac and by E 9.5 can be detected in the hindbrain and by E11.5 can be seen in the ventricular layer of the neuroepithelium in brain and spinal cord (Boudjelal et al., 1997; Ow et al., 2014). At E20 both *Bhlhe40* and *Bhlhe41* mRNAs are barely detected in whole brain RNA extracts, whose levels increase from P5 to P15, with maximal expression seen in adults (P90). In adult animals, *Bhlhe40* has wide tissue expression, namely: brain, kidney, liver, uterus, muscle, lung, gut, and heart, with low level expression in the spleen. By comparison, *Bhlhe41* mRNA expression is limited to the brain, muscle, heart, and weak expression in the lung. Taken together, both *Bhlhe40* and *Bhlhe41* are expressed in brain, with *Bhlhe40* being more ubiquitously

expressed than and *Bhlhe41* (Rossner et al., 1997). In the hippocampus specifically, *Bhlhe40* and *Bhlhe41* have partially overlapping expression patterns. Both transcripts are expressed in CA1, while only *Bhlhe40* is expressed in the subiculum and only *Bhlhe41* is expressed in the dentate gyrus. Interestingly, neither gene is expressed in CA2 or CA3. *Bhlhe40* and *Bhlhe41* gene expression is restricted to neurons (Rossner et al., 1997; Figure 3).

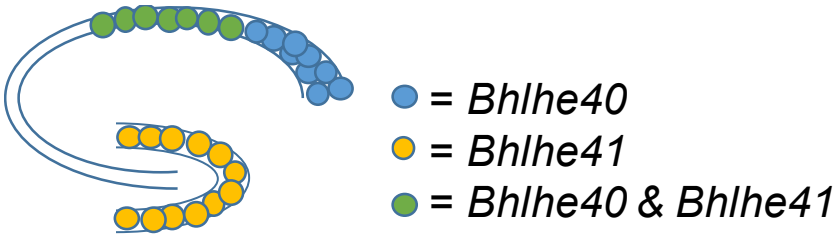

Figure 3. *Bhlhe40* and *Bhlhe41* hippocampal mRNA expression in neurons of adult rodents. The subiculum expresses only *Bhlhe40*, the dentate gyrus expresses only *Bhlhe41*, CA1 expresses both *Bhlhe40* and *Bhlhe41*, and CA2 and CA3 express neither transcripts.

Bhlhe40 and Energy

The carbohydrate response element binding protein (ChREBP), which is activated by glucose, upregulates *Bhlhe40* by binding to the carbohydrate response element (ChoRE) in the *Bhlhe40* promoter. Bhlhe40 protein then competes with ChREBP by binding to the ChoREs of *Bhlhe40* as well as for *fatty acid synthase* and *liver-type pyruvate kinase* (Iizuka and Horikawa, 2008). ChoREs consist of two E-boxes (Shih et al., 1995), which are favorable sites for Bhlhe40-mediated repression (St-Pierre et al., 2002). Bhlhe40 represses expression of peroxisome-proliferator-activated receptor γ co-

activator 1α, a transcriptional co-activator that promotes oxidative metabolism (Hsiao et al., 2009), which in the brain is involved in the maintenance of synapses (Cheng et al., 2012). Insulin also activates *Bhlhe40* gene expression via a phosphoinositide 3-kinase pathway (Yamada et al., 2003); however, the role of Bhlhe40 and insulin signaling has not been fully elucidated. Taken together, this suggests that Bhlhe40 regulates glucose-mediated metabolic pathways and suggests a possible role in neuronal activity, due to the high energy demands in neurons (Lutas and Yellen, 2013).

Bhlhe40 in Hypoxia and DNA Damage

Bhlhe40 transcription can be activated by hypoxia via the hypoxia inducible factor 1 (HIF-1; Ivanova et al., 2001; Ow et al., 2014), vitamin D (Seuter et al., 2013), insulin (Yamada et al., 2003), gonadotropins, parathyroid hormone, infection, and circadian rhythms (Yamada et al., 2005). Notably, Bhlhe40 protein levels are upregulated by hypoxia in cultured hippocampal neurons (Chen et al., 2011) and in an animal model of transient forebrain ischemia *Bhlhe40* transcripts were found to be more than three-fold upregulated in the hippocampus (Nagata et al., 2004).

At baseline, Bhlhe40 protein is short-lived due to proteasome degradation via the $SCF^{\beta TrCP}$ ubiquitin ligase. In response to DNA damage, and perhaps other Bhlhe40-inducing stimuli, however, Bhlhe40 is deubiquitylated by USP17, thereby extending its lifespan (Kim et al., 2014). In response to DNA damage, Bhlhe40 interacts with p53 at the macrophage inhibitory cytokine-1 (MIC-1) promoter, thereby preventing p53-mediated upregulation of MIC-1, a cytokine that promotes apoptosis (Qian et al., 2012a).

Bhlhe40 also upregulates the expression of survivin, an anti-apoptotic protein (Li et al., 2006). Together, this suggests that Bhlhe40 is involved in the DNA damage response and may play a role in cell survival.

Bhlhe40 in Neuronal Activity

Bhlhe40 mRNA levels are upregulated in the hippocampus, most notably in the subiculum, within one hour following injection of the convulsant, kainic acid (KA; Rossner et al., 1997). HIF-1a, one of the subunits of the HIF-1 transcription factor, is upregulated in the hippocampus following seizure initiation (Gualtieri et al., 2013; Long et al., 2014) and *Bhlhe40* mRNA increases could therefore be mediated by seizure-induced HIF-1 activity (Ow et al., 2014). KA also induces DNA damage following KA-injection, however, this may not occur until 16-hours post-injection (Puttachary et al., 2015), therefore DNA damage could be upregulating *Bhlhe40* mRNA and protein later on, but is likely not responsible for the one-hour increase in *Bhlhe40* transcription noted in Rossner et al. (1997). Another possibility is that *Bhlhe40* mRNA is upregulated in response to neuronal activity. Supporting this notion, *Bhlhe40* null KO mice on a mixed genetic background (129, C57Bl/6, CD1; *Bhlhe40* KO-mix) were found to have increased seizure severity following KA injection as well as increased levels of *Bdnf* transcripts from promoter 4 (*Bdnf-4*), which is known to have activity-dependent expression (Jiang et al., 2008). In addition, it was found that treatment of cultured neurons with NMDA decreased Bhlhe40 binding to *Bdnf* promoter 4, indicating that Bhlhe40 is responsive to neuronal activity (Jiang et al., 2008). Together, the available data suggests that Bhlhe40

plays a role in regulating at least one gene involved in neuronal activity (Figure 4). It is therefore possible that Bhlhe40 regulates other genes involved in neuronal activity and that deletion of Bhlhe40 may alter the excitability landscape, leading to increased seizure susceptibility. Further, given the data to suggest Bhlhe40 in hippocampal neuronal activity, and in particular the responsiveness to NMDA treatment, it is likely that Bhlhe40 is involved in hippocampal synaptic plasticity and learning and memory.

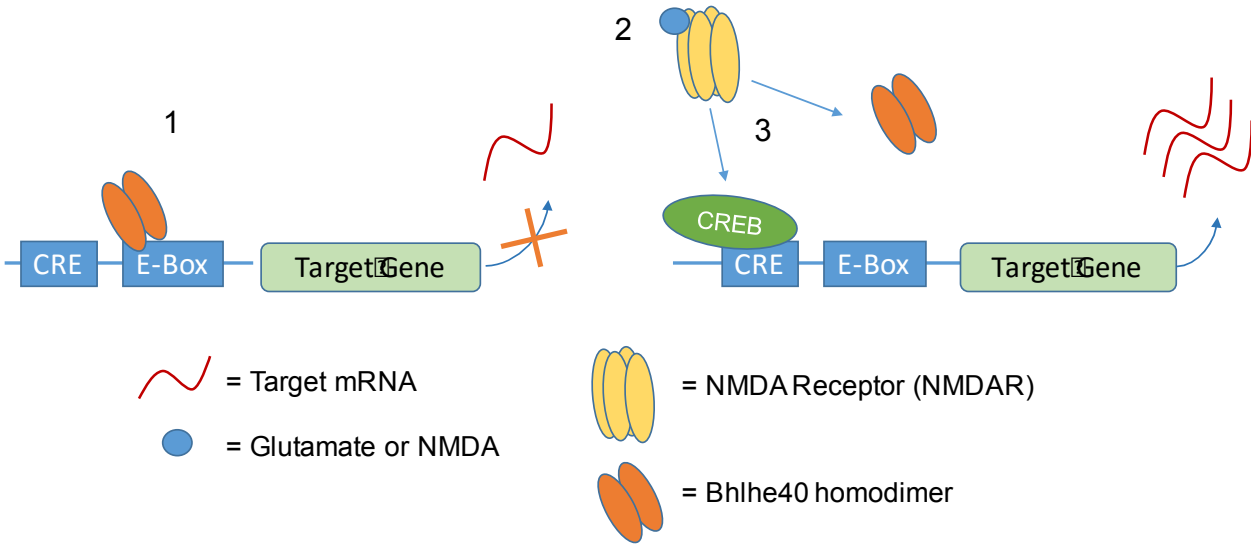

Figure 4. Proposed activity-dependent regulation of gene expression by Bhlhe40.
1) Bhlhe40 represses target gene transcription at baseline by E-box binding. 2) Glutamate or NMDA activate NMDA receptors (NMDARs). 3) Bhlhe40 is dislodged from its E-box and transcription is upregulated by cyclic AMP response element (CRE) binding protein (CREB).

Possible Electrophysiological and Behavioral Abnormalities in *Bhlhe40* KO Mice

After the publication of the Jiang et al. (2008) study, the *Bhlhe40* KO-mix mice were repeatedly backcrossed with C57Bl/6 mice at Jackson laboratories to generate a congenic *Bhlhe40* KO mouse (*Bhlhe40* KO) via speed congenics (Wong, 2002). C57Bl/6 is one of the most commonly used mouse strains in research (Fortin et al., 2001) and use of congenic mice serves to standardize genetic background (Rogner and Avner, 2003). It is therefore prudent to utilize the congenic C57Bl/6 *Bhlhe40* KO mouse model; however, differential effects between genetic backgrounds regarding seizure susceptibility may exist. Previously, C57Bl/6 mice were found to have less severe seizures and less seizure-induced cell death than the FVB strain of mice, or FVB and C57Bl/6 hybrids (Mohajeri et al., 2004). This indicates that the *Bhlhe40* KO mouse, while a more standardized model for the investigation of *Bhlhe40* gene function, may have less susceptibility to seizures than *Bhlhe40* KO-mix mice.

Changes in genetic background may also affect Bhlhe40 transcriptional activity. For example, change in any nucleotide in the class B E-box (CACGTG) would reduce Bhlhe40 binding affinity (St-Pierre et al., 2002). Further, a change in the spacing of promoter elements could also affect Bhlhe40 interactions with other transcription factors (Figure 2). For example, if the p53 response element is farther spaced from the Bhlhe40-bound E-box, then Bhlhe40 and p53 are less likely to interact (Qian et al., 2012b). This suggests the possibility that Bhlhe40 may have different transcriptional effects in the congenic background as opposed to the mixed genetic background, and *Bhlhe40* KO mice may therefore have a different transcriptome than *Bhlhe40* KO-mix mice.

Taking into consideration that *Bhlhe40* KO mice may be quite different than *Bhlhe40* KO-mix mice, I sought to elucidate the role of *Bhlhe40* gene deletion on synaptic plasticity and neuronal excitability using the *Bhlhe40* KO mice. Two hallmarks of seizures are neuronal hyper-excitability and network hyper-synchronization (Suzuki, 2013). Because of the potential role of Bhlhe40 in regulating genes involved in activity (Jiang et al., 2008) and because *Bhlhe40* is expressed only in CA1 and subiculum of the hippocampus (Rossner et al., 1997), it is possible that *Bhlhe40* deletion induces hyper-excitability in CA1 and subiculum neurons, but that this effect does not induce hippocampal network hyper-synchronization in *Bhlhe40* KO mice. For this reason, investigation into neuronal excitability on the single cell level, as well as behavioral seizures, will help elucidate the role of Bhlhe40 in neuronal excitability and seizure susceptibility (Figure 5).

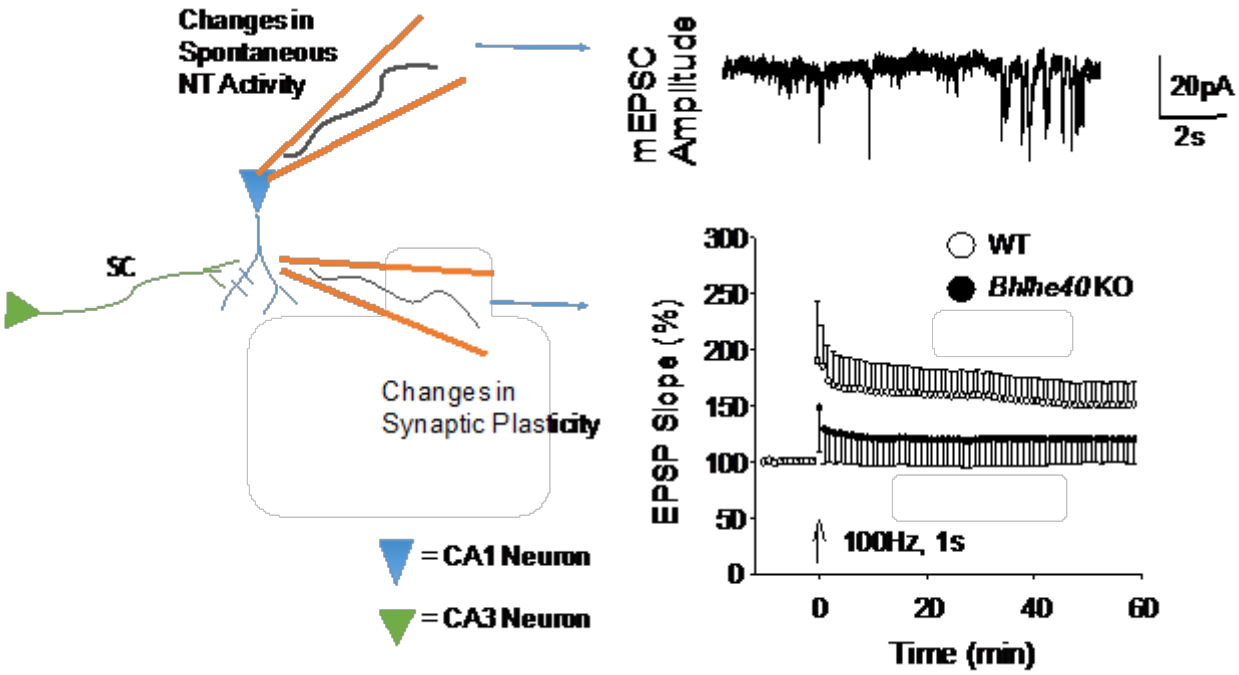

Figure 5. Potential changes in neuronal excitability and synaptic plasticity due to loss of Bhlhe40 transcriptional regulation.
Left) Hippocampal circuit showing an intracellular electrode (top orange lines) measuring spontaneous neurotransmitter release and an extracellular electrode (bottom orange lines) measuring synaptic strength at Schaffer Collateral (SC)-CA1 synapses. Right) An example of increased response to spontaneous neurotransmitter release measured as miniature excitatory post-synaptic current (mEPSC) amplitude and decreased synaptic strengthening at *Bhlhe40* KO SC-CA1 synapses in response to high frequency (100Hz) stimulation of SCs.

The original work with the *Bhlhe40* KO-mix mice suggests that Bhlhe40 plays a role in the regulation of activity-dependent genes, along with NMDA receptors (NMDARs) and CREB (cyclic AMP response element binding protein; Figure 4; Jiang et al., 2008). If this is the case, then *Bhlhe40* gene deletion may cause an upregulation of activity-dependent genes even without NMDAR-activation. NMDAR activation and transcription by CREB are involved in synaptic plasticity and learning (Shipton and

Paulsen, 2013; Barco and Marie, 2011). Therefore, *Bhlhe40* KO mice may have disrupted synaptic plasticity, as well as learning and memory (Figure 5).

The following chapters will explore the consequence of *Bhlhe40* gene deletion in a pure congenic C57Bl/6 genetic background on neuronal excitability, seizure susceptibility, synaptic plasticity, learning and memory, and gene expression. In addition to learning and memory, which is evaluated using the Morris water maze, a hippocampal-dependent task (Middei et al., 2014), the open field task is used as a measure of exploratory activity that may indicate differences in anxiety (Bailey and Crawley, 2009) and amygdala (Belzung et al., 2014) function.

CHAPTER TWO: BASIC HELIX LOOP HELIX ENHANCER 40 NULL MICE HAVE IMPAIRED SYNAPTIC PLASTICITY, ENHANCED NEURONAL EXCITABILITY, AND DECREASED EXPRESSION OF INSULIN DEGRADING ENZYME

Wrote Chapter: Kelly Hamilton

Edited Chapter: Robert Lipsky

Collected Data: Kelly Hamilton, Yue Wang, Sophia Raefsky, Sean Berkowitz, Ryan Spangler, Caitlin Suire

Analyzed Data: Kelly Hamilton, Yue Wang

Citation: Kelly A. Hamilton, Yue Wang, Sophia Raefsky, Sean Berkowitz, Ryan Spangler, Caitlin Suire, Simonetta Camandola, Mark P. Mattson*, Robert H. Lipsky*. *In Preparation*

*Authors contributed equally.

Abstract

Basic helix loop helix enhancer 40 (Bhlhe40) is a transcription factor expressed in rodent hippocampus, however, its role in neuronal function is not well understood. Here, we used *Bhlhe40* null mice on a congenic C57Bl6/J background (*Bhlhe40* KO) to investigate the impact of Bhlhe40 on neuronal excitability and synaptic plasticity. A whole genome expression array predicted that *Bhlhe40* KO mice have up-regulated insulin-related pathways and down-regulated neuronal signaling-related pathways in the

hippocampus. We validated that insulin degrading enzyme mRNA (*Ide*) and IDE protein are significantly downregulated in *Bhlhe40* KO hippocampi. No significant difference was observed in hippocampal insulin levels. In hippocampal slices, we found CA1 neurons have increased miniature excitatory post-synaptic current (mEPSC) amplitude and decreased inhibitory post-synaptic current (IPSC) amplitude, indicating hyper-excitability in CA1 neurons in *Bhlhe40* KO mice. At CA1 synapses, we found a reduction in long term potentiation (LTP) and long term depression (LTD), indicating an impairment in hippocampal synaptic plasticity in *Bhlhe40* KO hippocampal slices. *Bhlhe40* KO mice displayed no difference in seizure response to the convulsant kainic acid (KA) relative to controls. We found that while *Bhlhe40* KO mice have decreased exploratory behavior they do not display alterations in spatial learning and memory. Together this suggests that Bhlhe40 plays a role in modulating neuronal excitability and synaptic plasticity *ex vivo*, however, Bhlhe40 alone does not play a significant role in seizure susceptibility and learning and memory *in vivo*. In addition, based on the reduction in IDE protein levels in these mice, there may be dysregulation of other known IDE substrates, namely insulin growth factor (Igf)1, Igf2, and Amyloid beta (Aβ).

Introduction

Bhlhe40 (also known as Clast5, Stra13, Sharp2, Dec1, Eip1, Cr-8, and Bhlhb2) is a transcription factor that 1) directly represses gene expression via binding to class B E-box sequences (CACGTG; St-Pierre et al., 2002), 2) directly activates gene expression by

binding to Sp1 sites (Li et al., 2006; Qian et al., 2014), and 3) indirectly regulates gene expression by interacting with basal transcription machinery, other transcription factors, or histone modifiers (Yamada and Miyamoto, 2005; Qian et al., 2008; Ow et al., 2014). Bhlhe40 and its sister protein, Bhlhe41, both have high affinities for class B E-boxes, and both factors regulate transcription as homodimers or heterodimers with each other, due to the high degree of similarity in the Bhlhe40 and Bhlhe41 basic helix-loop-helix domains (Kato et al., 2014). However, Bhlhe40 and Bhlhe41 interact with different proteins due to differences in their C-termini (Ow et al., 2014; Kato et al., 2014), therefore differential effects on gene expression are to be expected.

Bhlhe40 is highly expressed in mouse brain, specifically in hippocampus, cortex and is involved in a number of essential functions such as circadian rhythms, immune function, hypoxia, DNA damage responses, and metabolism (Boudjelal et al., 1997; Rossner et al., 1997; Yamada and Miyamoto, 2005; Kato et al., 2014; Ow et al., 2014). Rats injected with the convulsant KA had increased *Bhlhe40* expression in hippocampus and cortex in neuronal cell body layers (CA1 and Subiculum of the hippocampal formation and layer 5 of cortex; Rossner et al., 1997). In a mixed background line of mice deficient for *Bhlhe40* (*Bhlhe40* KO-mix), a single intraperitoneal injection of KA resulted in enhanced seizure severity compared to littermate control mice containing the gene (Jiang et al., 2008). *Bhlhe40* KO-mix mice had enhanced BDNF gene expression from one of the known activity-dependent promoters of the BDNF gene, promoter 4, and also had more-severe KA-induced seizures than normal littermates. Jiang and colleagues therefore postulated that the increase in seizure severity in *Bhlhe40* KO-mix mice could

be due to increased BDNF gene expression, supporting the BDNF hypothesis for epilepsy (Binder et al., 2001; Scharfman, 2005). In addition, they found that Bhlhe40 occupancy of an E-box binding site on the fourth promoter of the BDNF gene was lost upon NMDA receptor (NMDAR) activation, suggesting that Bhlhe40 inhibits at least one NMDAR signaling target at baseline and that Bhlhe40 may have a role in neuronal excitability (Jiang et al., 2008). Here, using a line of *Bhlhe40* null mice on a pure C57Bl/6 background (*Bhlhe40* KO) we investigated changes in gene expression and neuronal activity in hippocampus.

Materials and Methods

Mice

Use of *Bhlhe40* KO mice were generated as described previously (Jiang et al., 2008) and backcrossed for six generations into the C57Bl/6 background strain to generate the congenic mouse model. Animals in this study were housed at the National Institute on Aging facility on a 12hr light/dark cycle and allowed free access to food and water. Experiments on pups used mixed gender mice, while experiments on adults used only male mice to avoid variances in hormonal regulation. This research was approved by the National Institute on Aging Animal Care and Use Committee and was performed according to guidelines in the NIH Guide for the Care and Use of Laboratory Animals.

Gene Expression

Brain extraction and fresh tissue dissection: Animals were fasted overnight prior to isoflurane anesthesia, decapitation, and brain removal. On ice, the hippocampus was isolated from the brain as described previously (Mathis et al., 2011). Cortex and cerebellum were then dissected. Isolated tissue was snap frozen on dry ice then stored at -80˚C until later use.

Gene Expression Array Biological Sample Processing: Hippocampus, cortex, and cerebellum were isolated from naïve 3-5 month old WT (n=4) and *Bhlhe40* KO (n=4) between 10:30 am and 1 pm. RNA was extracted from brain tissue samples using an electronic tissue homogenizer and 1mL Qiazol followed by spin column isolation according to manufacturer protocols (Qiagen; Cat#: 74104). Total RNA was quality-controlled for by using the Agilent Bioanalyzer RNA 6000 Chip (Agilent, Santa Clara, CA). 500 ng of RNA was then amplified to create biotinylated antisense RNA via the Illumina® TotalPrepTM RNA amplification kit according to the manufacturer's instructions. 750 ng of biotinylated antisense RNA was hybridized overnight to mouse Ref8 v2 BeadChip microarrays (Illumina, San Diego, CA). Following post-hybridization rinses, arrays were incubated with streptavidin-conjugated Cy3, and scanned at 0.53 microns using an Illumina iScan scanner. Hybridization intensity data were extracted from the scanned images, and evaluated using Illumina GenomeStudio software, V2011.1.

Gene Expression Array Significance Determination: Raw microarray florescent signal data were filtered by the detection p-value and Z normalization to obtain

normalized probe signals. Sample quality was first analyzed by scatter plot, principal component analysis, and gene sample hierarchy clustering to exclude possible outliers. One-way ANOVA test on the sample groups were used to eliminate the probes/genes with larger variances within each comparing group. ANOVA p-values less than 0.05 were adopted for each probe/gene as a global quality filter. Genes were determined to be differentially expressed after calculating the gene expression change scale by Z-ratio, which indicates the fold-difference between experimental groups, and correcting for multiple comparison error level by false discovery rate (FDR), which controls for the expected proportion of false rejected hypotheses. Individual genes with p values less than 0.05 and an FDR less than 0.3 were considered significantly changed. Hierarchy clustering, K-means clustering, and principal components analysis (PCA) were performed to identify patterns within groups and probes affected by various experimental factor effects.

Gene Expression Array Pathway Analysis: The parameterized analysis of gene enrichment (PAGE) algorithm was employed for gene set enrichment analysis by using all of the genes in each sample as input against and the data set supplied by Gene Ontology Institute and MIT Broad Institute pathway gene set. For each relevant comparison, the lists of differentially expressed genes and Z ratios were entered into the PAGE Pathway Analysis software to organize them according to known biological pathways. The Enrichment Z-scores for each functional grouping were calculated based on the chance of mRNA abundance changes predicting these interactions and networks by Z-test. All pathways considered significant have at least have three genes found in the

microarray gene set. Gene Ontology terms were required for each gene to have a p value less than 0.05 and an FDR less than 0.3. A more stringent criteria was used for analysis of canonical pathways, requiring a p value less than 0.01 and an FDR less than 0.1. MIAME compliant Gene Expression Array data has been deposited to the NCBI Gene Expression Omnibus: http://www.ncbi.nlm.nih.gov/geo/

QRT-PCR: MRNA from 4-5 month old WT (n=8) and *Bhlhe40* KO (n=8) mice, P18-20 naïve WT (n=9) and *Bhlhe40* KO (n=9) pups, and 4-7 month old post-behaviorally trained WT (n=6) and *Bhlhe40* KO (n=6) mice were extracted as describe above. All tissue dissections in adult animals were performed between 10:30 am and 1 pm. In the gene expression experiment using P18-P20 pups, we sacrificed animals at morning (9 am), afternoon (2 pm), and evening (9 pm) to test for circadian variation in Bhlhe40 candidate target genes. MRNA from these samples were reverse transcribed to cDNA using Superscript III First-Strand Synthesis SuperMix (Invitrogen; Cat#: 18080400). CDNA was amplified using Sybr green 2X master mix (Applied Biosystems; Cat#: 4309155) with intron-spanning primers designed using primer blast (NCBI); thermal cycling: 95˚C 10min then cycle 95˚C 1min, 72˚C 1min, 65˚C 1min, 40 times; followed by a melt curve from 70.0˚C to 90.1˚C with a read every 0.2˚C. All primers were intron-spanning with the exception of *Bdnf4*. *Bdnf1* and *Bdnf4* primers were identical to those used in the prior study (Jiang et al., 2008) for replication reasons. Only primer pairs that generated products with a single peak on the melt curve were used in the analysis. The comparative Ct method was used to determine the normalized changes of

the target gene relative to a calibrator reference. Table 1 shows primer sequences of genes tested and an *Hprt* control.

Table 1 QRT-PCR Primers

Gene	Forward Primer	Reverse Primer	Nucleotide Ref Seq
Ap2s1	TCGAGGCCATCCACAACTTC	ACCACCGTGTAAACCTTGTAGA	NM_198613.2
Arntl	TCGCAAGAGGAAAGGCAGTG	ATTTTGTCCCGACGCCTCTT	NM_007489.4
Atp6V0E	ATACCACGGCCTTACTGTGC	GTCTGCGACCTCAGTGCCTA	NM_025272.2
Bdnf 1	AAGCCGAACTTCTCACATGATGA	TGCAACCGAAGTATGAAATAACCATAG	NM_007540.4
Bdnf 4	CTGCCTAGATCAAATGGAGCTTCT	GGAAATTGCATGGCGGAGGTAA	NM_001048141.1
Bhlhe41	CCAAAAGGAGCTTGAAGCGAG	ACCGGCGATTTCAGAGAGC	NM_024469.2
Cacna2d1	ATTTGGACGCCCTGGAACTG	GCTCCTTTGGCTGAAGATTTGG	NM_001110845.1
Cacnb4	GAGGGCTGTGAGATTGGCTT	GAGGAATGTGCTCCGTCACT	NM_001285427.1
Camk1d	CTCGACACCCATGGATTGCT	ACTACAGAGCGTGGAAGGTG	NM_177343.4
Chl1	GTAGAGGTACTTGTGCCGGG	TCACTGTCGCTGTATTCACCA	NM_007697.2
Clcn3	ATCTGGCAGTTGTGCCTAGC	TCACACCACCTAAGCACGC	NM_007711.3
Clock	CCACAAGGCATGTCACAGTTTC	TTGCTGTATCATGTGCTGGC	NM_007715.6
Dbi	CGCTTTCGGCATCCGTATCA	GAAGTCCCTTTCAGCTTGTTCC	NM_007830.4
Dbp	CGCGCAGGCTTGACA	CAGGGCGTTTTCCTTCTCCA	NM_016974.3
Gabarap	GTGCCTTCTGATCTTACAGTTGGTC	ACGCTTTCATCACTGTAGGCA	NM_019749.4
Gabbr1	AGTCGCTGTGTCCGAATCTG	TCTGAGTGTGGCGTTCGATT	NM_019439.3
Gabrg2	CATCTCTGAGTGACGGGACC	GGTTTCACTCCGATGTCAGGT	NM_008073.3
Gatad2B	TGTTTAAGGGGAAAGGCATGG	TGGTTGCTGAACGGATGACA	NM_139304.1
Glud1	GTGGTCGATGTACCGTTTGG	ATGGTGCTGGCATAGGTGTC	NM_008133.4
GNA13	ATGAGGGTGCTGGTAGATGC	TGTGATGGAATGTAATCCGGT	NM_010303.3
Gria1	GGGAATGTGGAAGCAAGGACT	AAACAGAAACCCTTCATCCGCT	NM_008165.4
Gria2	AGACTACGACGACTCCCTGG	ACTTGAACCTGCTTGAGGGC	NM_001039195.1
Gria3	CTCCAAGATCACTTTCTGGGC	TGGCTCTGCGGATTTCATGT	NM_001290451.1
Ide	GACAGAGGAGGCGTTCCAAA	CTTCAGGTTGTGGCAAGGGT	NM_031156.3
Kcnab1	TGGAGATCATGGAAGCCTACTC	AGAACTTTCTGGCACCCCAT	NM_010597.4
Kcnab3	TATGAGCACGGCGTAAACCT	TAGCTTGATCTCCTCCAGCCT	NM_010599.4
Kcnd2	CATGACAACACTGGGGTATGG	GCATTTGCACTCCCGCTTTT	NM_019697.3
Kcnh1	GACGACTCCTGCAAAGGTTGG	TAGGATGATGTGAGGGGGTGT	NM_010600.3
Kcnh2	GATCCTGCGGGGTGATGTC	CATGTTGGTATCTCGAAGGTTGAA	NM_013569.2
Kcnma1	GGGTGATGATATCCGCCCAG	GTTGGCTGCAATAAACCGCA	NM_001253378.1
Mapk1	CCCAAATGCTGACTCCAAAGC	AGCCCTTGTCCTGACCAATTTA	NM_011949.3
MOBP	TGAGAGCAAGACAAGCGGAG	TGGCACGGCGGCTAGT	NM_001039365.2
Mrps21	GACAGTGATGGTTCAGGAGGG	GCGGCAAGGCTTCTCATAGTA	NM_078479.3
NdufB5	CGAAGACTGTCGCTCCTGT	AAATTCCGGGCGATCCATCT	NM_025316.2
NdufC1	GGATTTATCTCATCCAAACACACAA	GGTGAATCCAGAGGAAGGACTG	NM_025523.1
Ngfrap1	AGGGATAGGCCCAGAATAGCA	ACCCGTCATTCATCTGCCTG	NM_009750.2
NPY	CCCGCCACGATGCTAGGTAA	TTGTTCTGGGGGCGTTTTCT	NM_023456.3
NTrk3	CGCCAGCATCAACATTACGG	TGCTCCAGTCTCAATTCCCG	NM_182809.2
PDE1A	AGGAATGCTTGTCCTAGCCG	GTCCAGCAGTCTTCTTGTCTCA	NM_016744.4
Per1	GAAACGGCAAGCGGATGGAG	TGTGAGTTTGTACTCTTGCTGC	NM_011065.4
Ppargc1a	GCTCAAGCCAAACCAACAACT	GGCCCTTTCTTGGTGGAGTG	NM_008904.2
PPP1CB	CTCATCAGGTGGTGGAAGACG	CTTCGGTGGATTAGCTGTTCG	NM_172707.3
PPP3CA	GATGGATTTGACGGAGCCAC	TCAGCCTCAATAGCCTCAACA	NM_008913.5
Rabac1	CATCCTGTACTGCGTGGTGA	AGCGTGGGAGCCTATGAGTA	NM_010261.2
Rac3	GCTTCGGCCACTCTCCTATC	GACGGAACCAATCTCTCGGG	NM_133223.4
Rcor1	CGACTTCGATCCTGCCAAAC	CTCCATGTTGTACCCGTGCT	NM_198023.2
Rims1	GGGTCTCAAGGTGGTTGGAG	GGCAGGGGTTTACCATTCCA	NM_001012624.1
Scn1a	GGTTACTCTGAACTCGGGGC	AGCCCTTAAATGTGGCAACT	NM_018733.2
Scn3b	AATACCCCTGCGAGTCACTG	GGTAGTCAGACGCATTTTCCTG	NM_001286614.1
Scn8a	GTGTCGTGTGGCCCATAAAC	GCCGCTCGTAAGGTCAGC	NM_011323.3
Snx14	CCAAATTCAACAGAAGCACACAA	GCAGCAAGGTTTCGAGGAGT	NM_172926.3
Sod1	CTTCGAGCAGAAGGCAAGCG	AGTCACATTGCCCAGGTCTC	NM_011434.1
Sod2	GAACAATCTCAACGCCACCG	CCAGCAACTCTCCTTTGGGTT	NM_013671.3
Stmn1	CGACATGGCATCTTCTGATATTC	GAGCACCTCCTTCTCATGCT	NM_019641.4
Syn2	ACCAAGTGGAGGACAGACAAC	GACTTGTTTTGGACCTACTGCAA	NM_013681.3
Syngr1	TTCGACCCCTACACCCTGG	AAGCAGAAACCCACGAACCA	NM_207708.1
Timm8B	CGGACGAAGCGGAGTTACAA	TATGGCCTACTGCCCTCCTT	NM_013897.2
UQCRB	TCTCAGGTCAAAATGGCGGG	ATCATCTCGCATTAACCCCAGT	NM_026219.1
HPRT (control)	CCTGCTGGATTACATTAAAGCACTG	CCTGAAGTACTCATTATAGTCAAGG	NM_013556.2

Western blot: Protein quantification by western blot was performed on hippocampi contralateral to the hippocampi from naïve 3-5 month old mice described above for qRT-PCR analysis. Brain hippocampi from WT (n=5) and *Bhlhe4*0 KO (n=5) were homogenized in RIPA buffer supplemented with a protease inhibitor cocktail (Roche; Cat#: 04693124001). 20 μg proteins were separated on 4-12% Bis-Tris Gel (Thermo; Cat#: NP0335BOX) and transferred onto 0.45μm nitrocellulose membranes (Thermo; Cat#: 88025). Membranes were blocked in 5% milk (Thermo; Cat#: 37530) for 1 hour then incubated with primary antibodies overnight at 4˚C. Following washes and incubation with the HRP-conjugated secondary antibody for 1 hour the immunoreactive bands were detected by chemiluminescence (Pierce; Cat#: 32106). Relative protein levels were determined by densitometry using Fiji (image J analysis). Levels of GAPDH were used as an internal loading control. The following antibodies were used in this study: rabbit anti-GluR1 (Abcam; Ab109450); mouse anti-GluR2 (Millipore; MAB397); rabbit anti-$GABA_BR1$ (Abcam; Ab166604); rabbit anti-Cacna2d1 (Novus Biologicals; NBP1-51198); rabbit anti-$GABA_A\gamma2$ (Novus Biologicals; NB300-151); rabbit anti-Gabarap (Protein Tech Group; 18723-1-AP); rabbit anti-Kctd12 (Protein Tech Group; 15523-1-AP); rabbit anti-Camk1d (Origene; TA309027); rabbit anti-IDE (Gene Tex; GTX111664); rabbit anti-Scn1a (Abcam; Ab24820); rat anti-Chl1(Millipore; MABN299); rabbit anti-Per1 (Novus Biologicals; NBP2-24589); rabbit anti-Bhlhe41 (Biorbyt; orb224120); rabbit anti-Clock (Biorbyt; orb235103); goat anti-GAPDH (Santa Cruz; sc-20357). HRP secondary antibodies for the corresponding species were used (Jackson Immunoresearch).

BDNF ELISAs: Six WT and six *Bhlhe40* KO single hippocampi from naïve 3-4 month old mice were homogenized in PBS, centrifuged at 1200 x g for 5min at 4˚C, then re-suspended the tissue pellet in 200µL M-PER buffer (Thermo Scientific cat#: 78501). Samples were analyzed using a mature BDNF ELISA kit (Promega; Cat#: G7611) and a pro-BDNF ELISA kit (Aviscera Bioscience; Cat#: SK00752-08) according to manufacturer protocols. Values were determined according to a linear standard curve and normalized by protein concentration by BCA (Pierce; Cat#: 23227).

Insulin ELISA: Seven WT and Seven *Bhlhe40* KO single hippocampi from behaviorally trained 4-7 month old mice were homogenized in 100µL M-PER buffer (Thermo Scientific cat#: 78501) with protease inhibitors (Roche; Cat#: 04693124001), centrifuged at 12,000 x g for 30 min at 4˚C, then supernatant was collected [14]. Insulin detection was performed via an insulin ELISA (EMD Millipore; Cat#: EZRMI-13K) according to the manufacturer protocol. Values were interpolated from the variable slope standard curve by non-linear regression (4-paramater logistic function; 4PL) using PRISM software (Graph Pad; Version 5.0) and normalized by protein concentration via BCA (Pierce; Cat#: 23227). Hippocampi from behaviorally trained mice were used for insulin quantification due to the strong and specific downregulation of *Ide* found by qRT-PCR in hippocampi from behaviorally trained *Bhlhe40* KO mice.

Electrophysiology

Acute Slice Preparation: Hippocampal slices were prepared using procedures described previously (Wang et al. 2009). Briefly, transverse slices of whole brain were

cut at a thickness of 350 μm, and were allowed to recover for 1-6 hours in a holding chamber in artificial cerebral spinal fluid (ACSF), bubbled with 95/5% (O_2/CO_2) at room temperature. 3-4 month old mice for field recordings and P12-21 pups for whole cell recordings.

Hippocampal CA1 field recordings from acute slices: Field potentials were recorded from CA1 stratum radiatum using glass electrodes (1-3 MΩ) filled with bubbled ACSF. Schaffer collaterals were stimulated using bipolar tungsten electrodes at 0.033Hz and 30μs duration. The stimulation intensity was set to 30-40% of the maximum EPSP amplitude. LTP was induced by high frequency stimulation (100Hz, 1s) and LTD was induced by low frequency stimulation (1Hz, 15min). The ACSF for field recordings contained 50μM picrotoxin to block $GABA_A$ activity. Slices were pre-selected for those with a steep input-output curve. During recording, slices were warmed to 30-32˚C.

Whole cell recordings from acute slices: Whole-cell miniature excitatory postsynaptic currents (mEPSCs) were recorded from CA1 pyramidal neurons (Zhang et al. 2011). The neurons were visualized by differential interference contrast microscopy using a 40X water immersion lens. Series resistance was 6 to 10 MΩ. The patch electrode (3-5 MΩ) contained (in mM): 125 $CsMeSO_3$; 2.5 CsCl; 0.2 EGTA, 7.7 TEA; 20 HEPES; 8 NaCl, 4 Mg-ATP; 0.3 Na-GTP; 5 QX-314; pH 7.2; the osmolality was 280-290 mmol/kg. Series voltage steps (20 mV and 150 ms) from –70 mV to +40 mV generated AMPA and NMDAR currents simultaneously (Stellwagen and Malenka, 2006). To avoid capacitance transients generated by the step effect on the current, there was a delay of 50 ms between the start of a step and pre-synaptic stimulation.

Data Analysis: Data were collected using an Axopatch 200B and MultiClamp 700B (Molecular Devices, Sunnyvale, CA) amplifier. Signals were filtered at 2 kHz, digitized at 10 kHz, and analyzed using pCLAMP 8 software (Molecular Devices). Data was presented as the mean ± SEM and statistical comparisons were made using non-paired t tests and Mann-Whitney Rank Sum Test.

Kainic Acid Injections

Behavioral Seizures: Six WT and six *Bhlhe40* KO 5 month mice were anesthetized by isoflurane and implanted with a cannula (23XX gauge cannula with 26TW gauge stylus; Vita Needle) to dorsal hippocampus (from Bregma: 1.8 mm posterior, 1.5 mm lateral, 2.0 mm advanced ventrally from the dura). Mice were allowed two weeks to recover, then infused with 200nL of 227 ng of KA (Abcam; Cat#: Ab120100; Batch Molecular Weight: 226.74;) in sterile 0.9% saline (Heinrich et al., 2006). Animals were video monitored for six hours for behavioral seizure analysis according to a seizure scale described previously (Liu et al., 1999). Briefly, stage 1 freezing behavior; stage 2, rigid posture and/or tail extension; stage 3, myoclonic jerks of head and brief twitching; stage 4, forelimb clonus and partial rearing; stage 5, forelimb clonus with rearing and falling; stage 6, tonic-clonic seizures. Additionally, stage 7 was denoted for one animal that died. Seizure activity was assessed for stage 2 and up to avoid falsely labeling normal pausing behavior as seizure activity. Notably all animals

were infused at the same time of day (12pm) with one *Bhlhe40* KO and one WT infused each day for six consecutive days, with the infusion order counterbalanced.

Seizure induced neuronal death: Three days after KA infusion mice were perfused with formalin and the brain removed. Following overnight fixation, the brains were washed with PBS and transferred to 30% sucrose solution for at least two days before sectioning at 40μm thickness on a sliding microtome. Sections were stained with 1% cresyl violet acetate solution to assess cell death. Specifically, cell death was assessed on cresyl violet stained sections at 10x magnification by measuring the intensity of the CA3 cell body layer relative to stratum radiatum intensity for background, and by measuring the thickness of the CA3 cell body layer at the genu to measure for cell loss and apoptotic swelling, respectively, using Fiji software. Cell death in area CA3 was quantified due to its inherent sensitivity to KA due to the high concentration of KA receptors and recurrent connections (Fisahn, 2005).

Telemetry: A separate set of adult 3-4 month old mice were implanted with cannulas (described above) as well as with a subcutaneous radio transmitter (Data Sciences International; F20-EET) connected to the surface of the primary motor cortex (from Bregma: 0.6 mm anterior, 1.7 mm lateral; El-Hayek et al., 2011; O'Niel et al., 2013) on the contralateral hemisphere to the cannula implanted to dorsal hippocampus. Animals were given three weeks to recover, and for the first five days were given twice daily injections of an antibiotic (Baytril) and a nonsteroidal anti-inflammatory drug (Carprofen), to prevent infection and discomfort. EEGs were recorded for 72 hours of baseline, 72 hours post infusion of 0.9% NaCl saline (solvent for KA), and 72 hours post

infusion of a low dose of KA (200 nL of 57 ng) to prevent any possible animal death and to prevent saturation of the EEG signal from high activity. Infusions were performed at the same time of day and counterbalanced as described above for behavioral animals. Power analysis was performed on EEG signals using Neuroscore software (Data Sciences International). Power bands for delta (1-4Hz) and Theta/Alpha (6-10Hz) were used as surrogate signals for behavioral seizures scaled 1-3 (freezing through forelimb clonus) and 4-6 (seizures with rearing/falling), respectively (Abdullah and Islam, 2012). Additionally, Gamma (30-50Hz) power was assessed as it is seen just prior to seizures as the result of intra-hippocampal KA infusion (Levesque and Avoli, 2013).

Behavior

Open Field: Individual mice were allowed to freely roam an enclosed 27.3cm x 27.3cm, height 20.3cm Open Field (Med Associates Inc.; ENV-510) for 30 minutes. The XY dimensions of the field were segmented into 16x16 segments [(0,0) to (16,16)] with the center region defined as (4,4) to (12,12) and the perimeter region equal to the whole field minus the center region. Activity Monitor Software (Version 4.0, Med Associates) recorded and tracked animal movements via a 16-beam infrared array.

Morris Water Maze: Starting the day after open field training, the same animals were trained for six days to find the hidden platform in the upper right quadrant of the Morris water maze (MWM) for initial training. The water temperature was set to 24˚C and non-toxic white paint was added to the water to obscure the submerged platform.

The training consisted of four 60 second trials. If the animal was unable to find the platform in 60 seconds during the training, the experimenter guided the animal to the platform and allowed the animal to stay on the platform for 15 seconds. Recollection of the platform location was assessed on probe trials performed at 4, 24, and 48 hours post training. Immediately following the 48-hour probe, a test for visual impairments and motivation was conducted by returning the platform to the pool in a different location than the animals were trained on and affixing a small blue flag to the platform to allow animals to easily see the platform and to escape. Seven days later (14 days after the start of MWM training), the above procedure was repeated, training the animals to the opposite platform location (lower left quadrant; MWM reversal task). No vision test followed the MWM reversal task. Video tracking software (ANY-maze) was used to track and analyze the animals' performance on the MWM. After the last probe trial animals were fasted overnight, euthanized, and hippocampi were isolated for gene expression measurements.

Results

Bhlhe40 KO mice have altered basal gene expression in cortex, hippocampus, and cerebellum

In order to gain insights on the roles played by Bhlhe40 in brain physiology we performed a whole genome expression array using hippocampal, cortical, and cerebellar

mRNA from naïve 4-month old WT and *Bhlhe40* KO mice (n=4 each). Although we expected minimal changes in the cerebellum due to its lower levels of *Bhlhe40* gene expression compared to hippocampus and cortex (Rossner et al., 1997), we surprisingly found that all three tissues had a high number of significant gene changes. Notably, changes in gene ontology from *Bhlhe40* gene deletion are unique in the hippocampus and hierarchical clustering revealed a cleaner separation pattern between *Bhlhe40* KO and WT hippocampus (Figure 6). These changes led us to focus on the gene changes in the hippocampus.

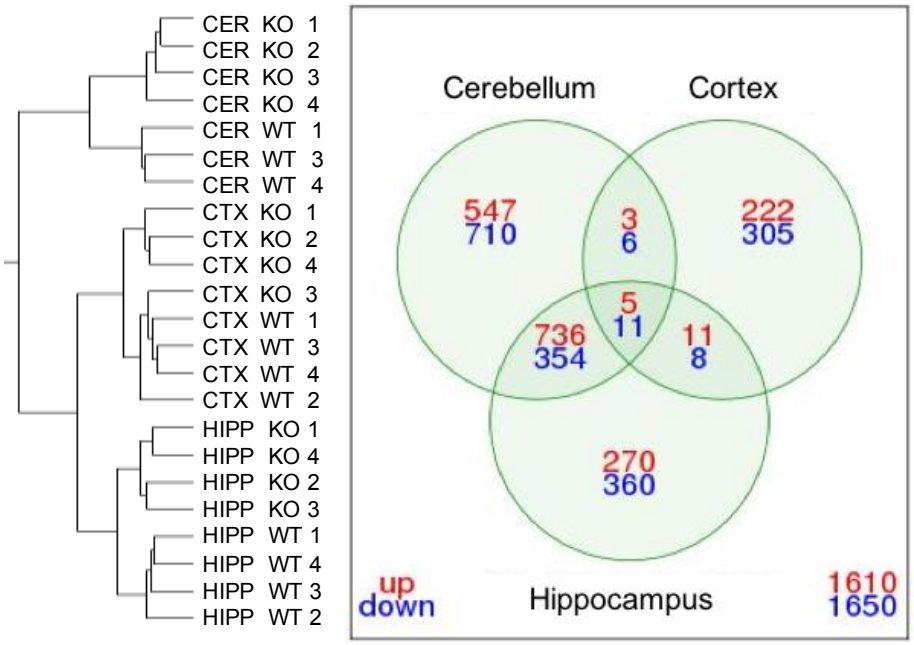

Figure 6. *Bhlhe40* KO mice have unique changes in gene expression in the central nervous system.
Unilateral hippocampus (HIPP), cortex (CTX), and cerebellum (CER) were isolated from naïve *Bhlhe40* KO and WT animals (n=4). MRNA was extracted and run on an Illumina whole genome expression array. Left) *Bhlhe40* KO and WT hippocampal gene expression had ideal clustering. One WT CER sample was removed as an outlier and one *Bhlhe40* KO CTX clustered with the WT samples, but was included in the analysis. Right) Gene ontology terms Venn Diagram.

In depth analysis showed an enrichment in pathway involved in energy metabolism and insulin signaling amongst the top 20 upregulated pathways in *Bhlhe40* KO hippocampus (e.g. Reactome electron transport chain, Reactome diabetes, Reactome insulin synthesis and secretion, and Reactome glucose regulation of insulin secretion; Figure 7). In addition, several pathways pertaining to neuronal signaling were included in the top 20 downregulated pathways (e.g. Kegg long term potentiation, Kegg long term depression, Reactome transmission across chemical synapses, and Reactome activation of NMDA receptor upon glutamate binding and postsynaptic events; Figure 7).

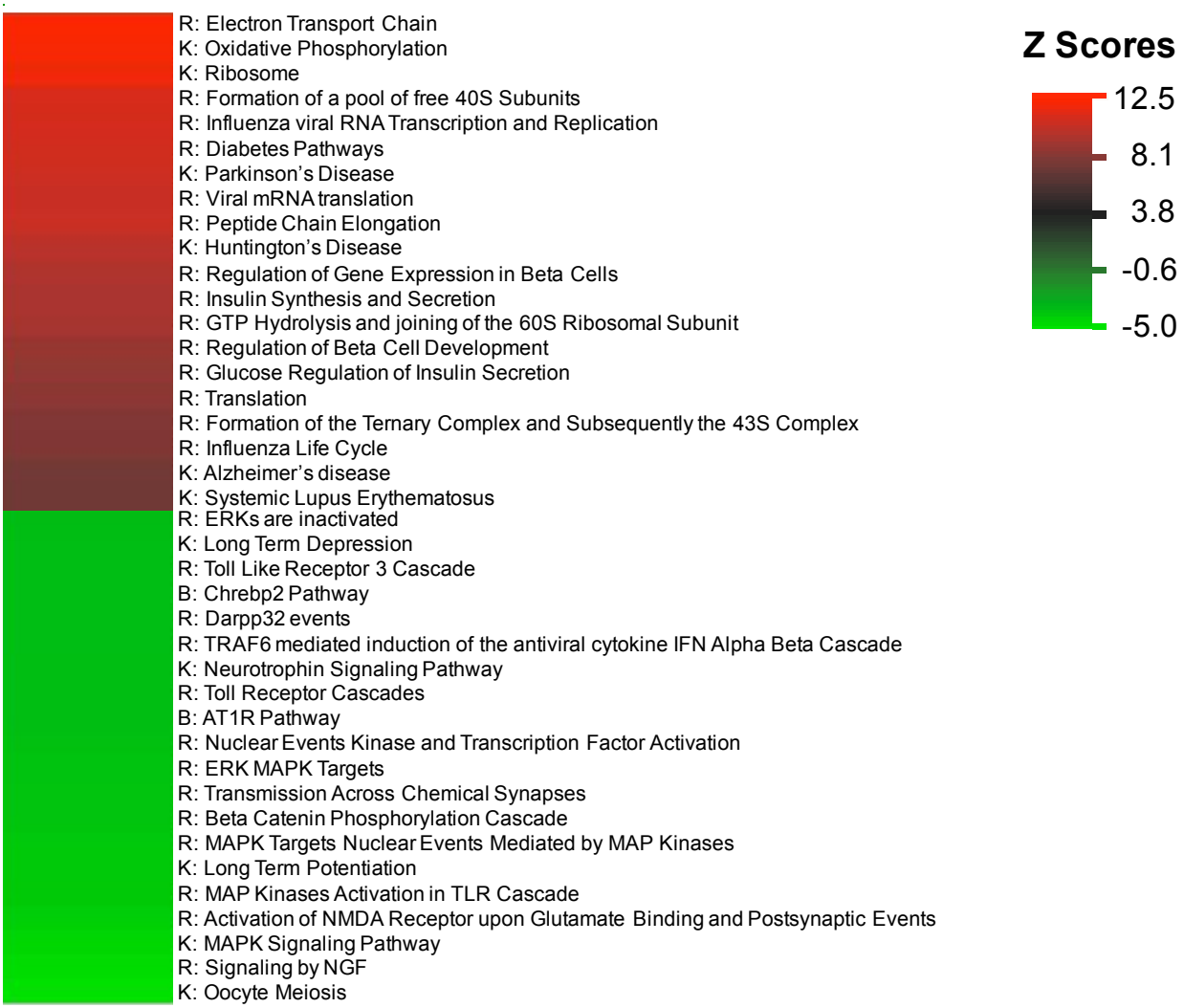

Figure 7. Changes in canonical pathways in *Bhlhe40* KO hippocampus.
Pathway analysis of a whole genome expression array on hippocampal genes identified several highly upregulated pathways in energy metabolism and downregulated pathways involved in synaptic activity in *Bhlhe40* KO mice compared to WT mice. The top 20 upregulated and top 20 downregulated pathways are shown, organized by Z score; n=4. R=Reactome; K=Kegg; B=Biocarta.

***Insulin degrading enzyme* transcripts are two-fold downregulated in *Bhlhe40* KO hippocampus**

We explored a number of genes predicted to be significantly changed in mRNA by quantitative reverse-transcription PCR (qRT-PCR) using the same four *Bhlhe40* KO and WT samples from the gene expression array plus another four samples (n=8; 3-5 months old). We identified the following genes encoding membrane receptors involved in neuronal signaling to be upregulated ($p<0.05$): Glutamate receptor 1 (*Gria1*), $GABA_B$ receptor 1 (*Gabbr1*), the potassium channel genes *Kcnh1, Kcnh2, Kcnab1*, sodium channel subunit 1a (*Scn1a*), and neurotrophic receptor tyrosine kinase 3 (*NTrk3*). Additionally, the GABA receptor associated protein (*Gabarap*) was upregulated, as were the circadian regulator genes *Clock* and *Dbp*, the cell adhesion molecule *Chl1*, and the protein kinase calmodulin kinase 1d (*Camk1d*). Only one gene was downregulated, Insulin Degrading Enzyme (*Ide*). *Bdnf1* and *Bdnf4* were run in an attempt to replicate findings on the *Bhlhe40* KO-mix mice, but were nonsignificant. There was no change in *Bdnf4* relative to *Bdnf1* levels. Only *Clock*, *NTrk3,* and *Ide* passed a Bonferroni correction for multiple comparisons (standard $\alpha=0.05$ adjusted for 36 gene comparisons WT v *Bhlhe40* KO unpaired t-test for each gene: $0.05/36 = 0.0014$; Figure 8).

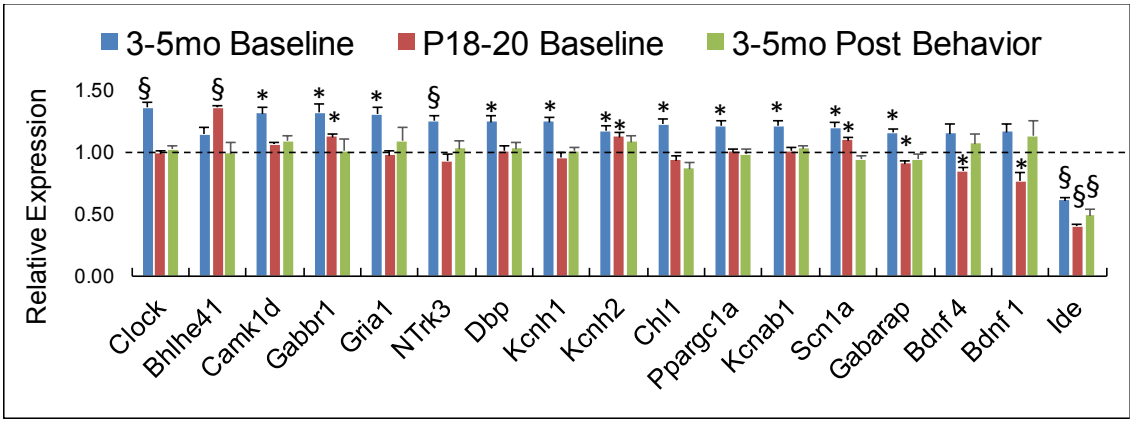

Figure 8. Validation of gene expression changes in *Bhlhe40* KO hippocampus.
Expression levels of *Bhlhe40* KO genes are expressed relative to WT (100% = dashed line). Gene expression within samples was normalized to the housekeeping gene *Hprt*. Unpaired t-tests were used to test for significance for each gene for adult groups and two-way ANOVA for each gene was used for P18-20 pups; *=$p<0.05$, §=$p<0.001$. $p<0.001$ passes a Bonferroni correction for multiple comparisons for each group. 3-5 month old baseline WT n=8, *Bhlhe40* KO n=8; P18-20 baseline WT n=9, *Bhlhe40* KO n=9; 4-7 month old post MWM WT n=6, *Bhlhe40* KO n=6. Error bars are standard error of the mean.

Bhlhe40 expression increases in the brain with age (Rossner et al., 1997) and so we investigated gene expression in *Bhlhe40* KO pups prior to weaning (P18-20) to determine if there were any differential effects on gene expression in this age group. Additionally, these pups were sacrificed at morning (n=3), afternoon (n=3), and evening (n=3) to test for circadian regulation of possible Bhlhe40 gene targets due to the known role of Bhlhe40 in the circadian system (Kato et al., 2014). We found no effect of circadian regulation on any of the genes compared (Figure 8 and Table 2; $p>0.05$ two-way ANOVA for interaction of genotype and time of day). We proceeded by combining all the P18-20 pups within a genotype for each between genotype comparison to determine the fold change (n=9). Significance was based on the p value for genotype effect on the two-way ANOVA for each gene. *Bhlhe41*, which was not significant in

adult transcripts, was upregulated in the pups ($p<0.001$). We noted that *Bdnf1* and *Bdnf4* mRNA levels were downregulated in the pups. *Bdnf4* was also not changed relative to *Bdnf1* in the *Bhlhe40* KO pups. Changes in gene expression in *Gabbr1*, *Kcnh2*, *Scn1a*, and *Ide* corroborated the findings in the adult mice. In the *Bhlhe40* KO pups, only *Bhlhe41* and *Ide* passed multiple comparison correction (standard $\alpha=0.05$ adjusted for 27 gene comparisons WT v *Bhlhe40* KO two-way ANOVA for each gene: 0.05/27 = 0.0019; Figure 8).

Lastly, to investigate if behavioral training on a hippocampal-dependent task (MWM) influenced hippocampal gene expression in *Bhlhe40* KO mice, we took RNA from adult *Bhlhe40* KO hippocampi that had been sacrificed following a MWM experiment. Investigating the same set of genes that were significant in either the naïve *Bhlhe40* KO adults or pups, we found only *Ide* to be changed, which passed multiple comparison correction (standard $\alpha=0.05$ adjusted for 41 gene comparisons WT v *Bhlhe40* KO unpaired t-test for each gene: 0.05/41 = 0.0012; Figure 8). In addition, several other genes were tested and found to be $p>0.05$ in each condition tested (Table 2). Not every gene was repeated when found to be insignificant at baseline in *Bhlhe40* KO adults and some genes were additionally tested in the post-behavior animals. Taken together, the most crucial finding from mRNA-level gene expression investigations was that *Ide* was the only gene that was consistently and significantly changed by *Bhlhe40* gene deletion in hippocampus across all comparison groups.

Table 2: Nonsignificant genes tested by qRT-PCR.
X indicates the condition(s) in which the genes were tested.

Genes p>0.05	3-5mo baseline	P18-20 Baseline	3-5mo Post Behavior
Cacna2d1	x	x	x
Gria2	x	x	x
Gria3	x	x	x
Per1	x	x	x
Gabrg2	x	x	
Kcnab3	x	x	
Scn3b	x	x	
Scn8a	x	x	
Snx14	x	x	
Arntl	x		
Cacnb4	x		
Clcn3	x		
Glud1	x		
Kcnd2	x		
Kcnma1	x		
Rabac1	x		
Stmn1	x		
Syngr1	x		
Ap2s1			x
Atp6V0E			x
Dbi			x
Gatad2B			x
GNA13			x
Mapk1			x
MOBP			x
Mrps21			x
NdufB5			x
NdufC1			x
Ngfrap1			x
NPY			x
PDE1A			x
PPP1CB			x
PPP3CA			x
Rac3			x
Rcor1			x
Rims1			x
Sod1			x
Sod2			x
Syn2bc			x
Timm8B			x
UQCRB			x

Insulin Degrading Enzyme protein is two-fold decreased in *Bhlhe40* KO hippocampus

We next investigated whether mRNA-level changes in *Bhlhe40* KO hippocampal gene expression translated to protein level changes. By western blotting we found a two-fold decrease in *Bhlhe40* KO hippocampal IDE protein levels relative to WT hippocampi

(from 3-5 month old naïve mice; Figure 9). In addition, Bhlhe41 was upregulated by 18% at the protein level ($p<0.05$), despite being insignificant in the adult animals on the mRNA level. Bhlhe41 protein blotting generated three bands, consistent with the two known sumoylation sites (Ow et al., 2014) and thus three possible sumoylation states (0, 1, and 2 sumoylations), which were all combined in the densitometry analysis in Fiji software to determine the total fold change. We also saw a 30% increase in Kctd12 protein ($p<0.05$). It should be noted that we decided not to analyze *Kctd12* mRNA levels by qRT-PCR because the gene contains only one exon and to ensure that only RNA levels were being measured, we used only intron-spanning primers. Scn1a protein levels were nonsignificant (Figure 9). Only the change in IDE protein levels passed multiple comparison correction (standard $\alpha=0.05$ adjusted for 14 WT v *Bhlhe40* KO unpaired t-tests for each protein: $0.05/14 = 0.0036$). We also examined differences between WT and *Bhlhe40* KO hippocampi for GluR1, $GABA_B$ Receptor 1 ($GABA_BR1$), Gabarap, Chl1, Clock, Camk1d, GluR2, $GABA_A$ receptor $\gamma2$ (Gabrg2), Cacna2d1, and Period1 (Per1) which did not have significant protein-level changes ($p>0.05$). GAPDH was used as a reference control for all proteins tested and was consistent between WT and *Bhlhe40* KO protein samples.

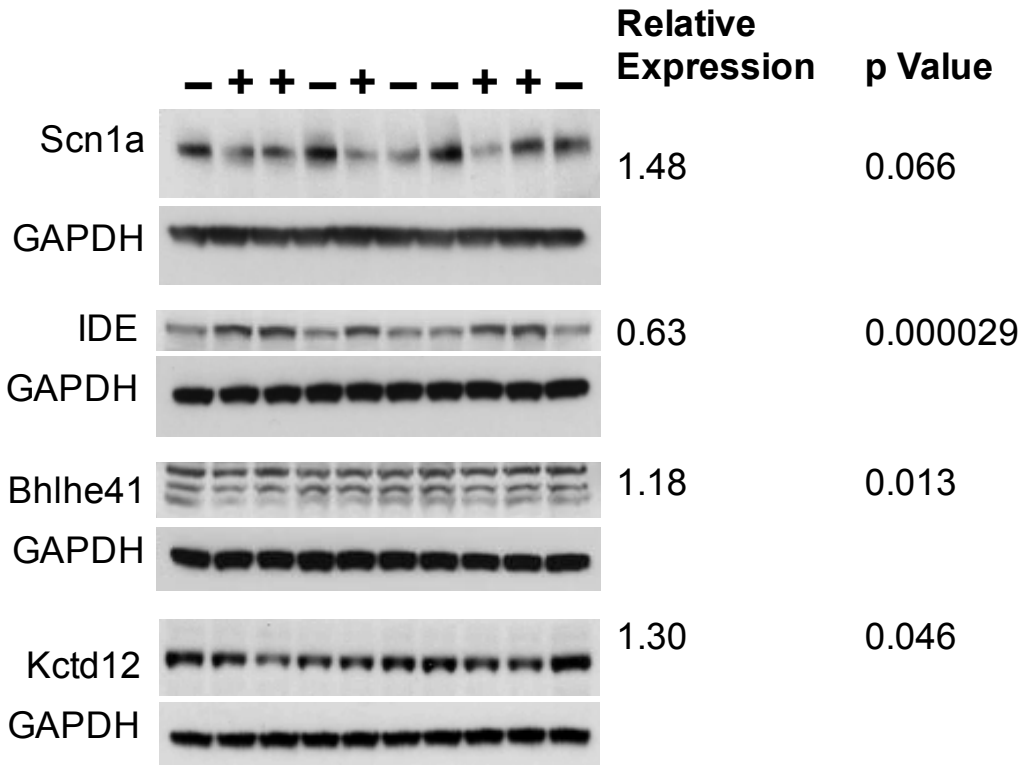

Figure 9. IDE protein is significantly reduced in *Bhlhe40* KO hippocampus.
Single hippocampi from six 3-5 month old WT and *Bhlhe40* KO mice were used for protein-level analysis by western blotting. Representative autoradiograms from WT (+) and *Bhlhe40* KO (-) samples are shown. Densitometry was performed using Fiji (Image J). Scn1a had a nonsignificant trend. For Bhlhe41, a triplet band was observed, presumably due to the three possible sumoylation states (0, 1, and 2 sumoylations). The relative expression for Bhlhe41 represents a combination of all three bands. Unpaired t-tests were used to test for significance changes for each protein. Additionally, GluR1, GluR2, $GABA_BR1$, Cacna2d1, Gabrg2, Gabarap, Chl1, Per1, Clock, and Camk1d were tested and found to be nonsignificant. Only IDE passes a Bonferroni correction for significance by multiple comparisons (0.05 standard alpha/14 proteins investigated gives an adjusted alpha level of 0.0036 for significance) and was thus considered the only significant change in protein level in *Bhlhe40* KO hippocampus.

Given the previous report that BDNF levels are elevated in *Bhlhe40* KO mice on a mixed genetic background (Jiang et al., 2008), we sought to determine if there was a difference in protein levels of mature BDNF or proBDNF in *Bhlhe40* KO hippocampus at baseline. Protein extracts from six WT and six *Bhlhe40* KO naïve 3-5 month old

unilateral hippocampi were run on independent ELISAs to assay for mature BDNF and proBDNF. There was no significant difference in either form of BDNF between *Bhlhe40* KO and WT hippocampi (Figure 10).

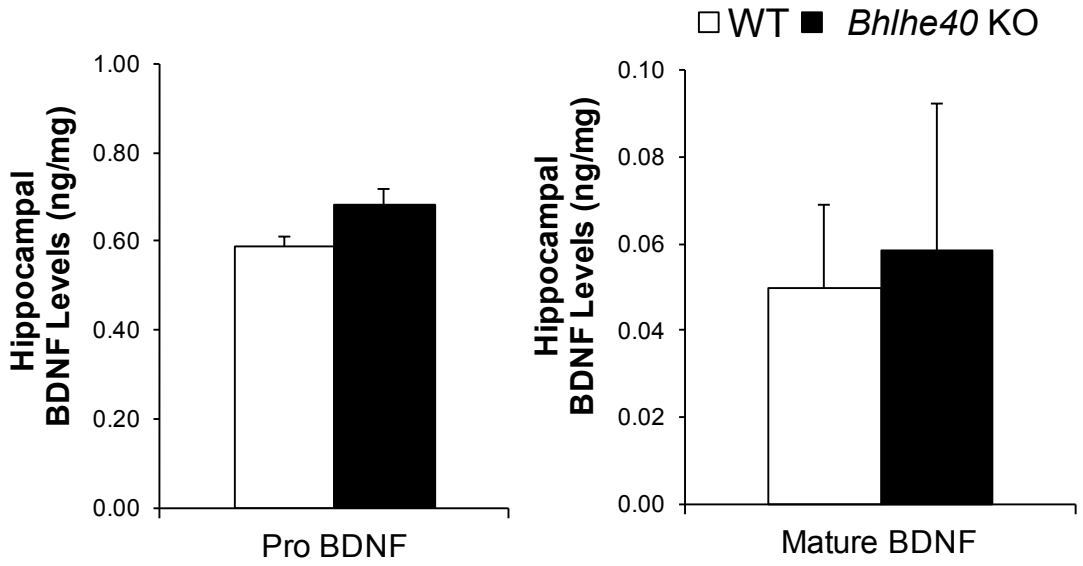

Figure 10. Pro- and mature-BDNF protein levels are not changed in *Bhlhe40* KO mice hippocampi.
Single hippocampi from six 3-5 month old naïve WT and *Bhlhe40* KO mice were used for BDNF quantification by ELISA. Pro BDNF and mature BDNF were tested for on independent ELISAs. BDNF levels are expressed in ng of BDNF relative to mg of total protein. Left) pro BDNF (unpaired t-test $p>0.05$); Right) mature BDNF (unpaired t-test $p>0.05$). Error bars are standard error of the mean.

Body weight, but not insulin levels, are altered in *Bhlhe40* KO mice

Given our findings of decreased IDE protein levels in *Bhlhe40* KO hippocampus, we wanted to determine if there was an increase in IDE substrate levels, namely insulin, in *Bhlhe40* KO mice via an insulin ELISA. We used seven WT and seven *Bhlhe40* KO

post-behavior trained mice, which indicated a significant and specific decrease in hippocampal *Ide* mRNA levels (Figure 8). Hippocampal insulin levels trended toward an increase (p=0.07), but were nonsignificant in *Bhlhe40* KO mice relative to WT controls (Figure 11). Interestingly, we found the *Bhlhe40* KO do not gain weight with age as do WT animals (comparing 29 WT and 29 *Bhlhe40* KO 3-4 month old animals vs. 14 WT and 17 *Bhlhe40* KO 5-6 month old animals; two-way ANOVA $p<0.05$; 5-6 month old animals unpaired t-test $p<0.01$).

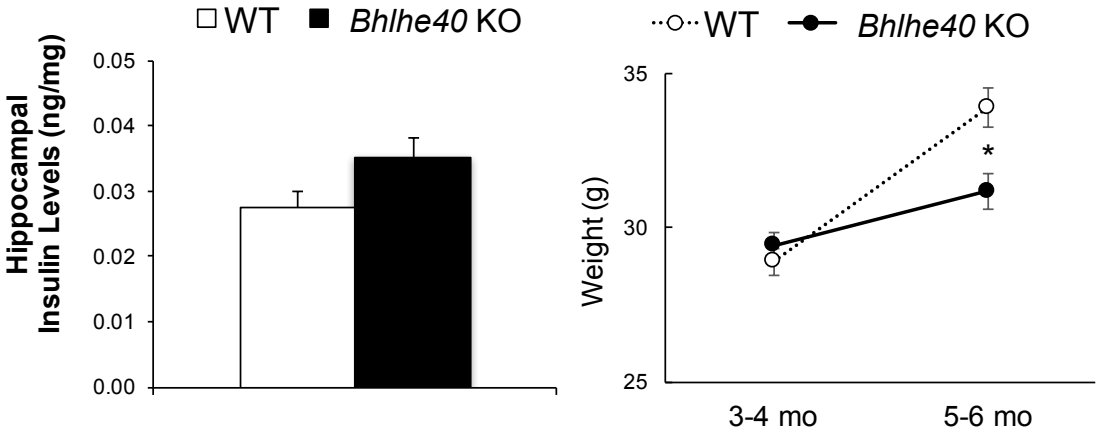

Figure 11. *Bhlhe40* KO mice have decreased weight gain with age and no change in hippocampal insulin levels.
Left) Single hippocampi from seven 4-7 month old WT and *Bhlhe40* KO mice post-behavior training were used for insulin quantification by ELISA. Insulin levels are expressed in ng of insulin relative to mg of total protein (insulin ELISA students t-test p= 0.07). Right) Baseline body weights at 3-4 months from WT (n=29) and *Bhlhe40* KO (n=29) mice and at 5-6 months from WT (n=14) and *Bhlhe40* KO (n=17) were compared. Two-way ANOVA $p<0.05$; unpaired t-test for 5-6 month old animals $p<0.01$. Error bars are standard error of the mean.

Bhlhe40 KO CA1 neurons are hyperexcitable

In single cell recordings in hippocampal slices we found that CA1 neurons from *Bhlhe40* KO mice have significantly reduced evoked IPSC amplitude in CA1 hippocampal neurons (Figure 12A; 14.4% decrease; $p<0.05$;). Additionally, mEPSC amplitude are significantly greater (Figure 12B; 40% increase; 5.4pA; $p<0.01$) than WT controls, however there was no difference in mEPSC frequency (data not shown). This suggests that the rate of spontaneous neurotransmitter release is not affected, but the post-synaptic response to a given quantal release is greater. This shows that *Bhlhe40* KO CA1 neurons have a greater excitatory response and a weaker inhibitory response, indicating an overall increase in neuronal excitability.

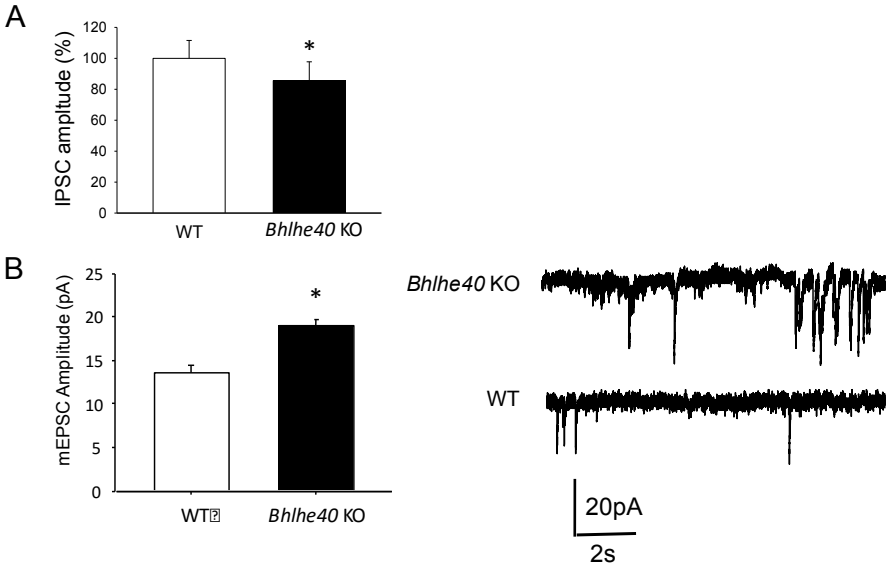

Figure 12. *Bhlhe40* KO mice have increased hippocampal excitability.
A) *Bhlhe40* KO mice have a 14.4% decrease in IPSC amplitude (*Bhlhe40* KO: 85.6 +/- 12.2, WT: 100 +/- 11.6); n=4 mice for each *Bhlhe40* KO (5 cells) and WT (6 cells). B) Left: *Bhlhe40* KO mice have a 40% increase in mEPSC amplitude, relative to WT levels (*Bhlhe40* KO: 18.99 +/-

0.69 pA, WT: 13.6 +/- 0.88 pA). Right: Example traces of mEPSCs from WT and *Bhlhe40* KO slices. Error bars are standard error of the mean; unpaired t-tests were used for both mEPSC and IPSC amplitude comparisons *Bhlhe40* KO hippocampal slices compared to WT slices; *=p<0.05.

Bhlhe40 KO hippocampal slices have reduced LTP and LTD

In field recordings from hippocampal area CA1 there was a significant reduction in both LTP (60% decrease; p<0.001; Figure 13C) after high frequency stimulation (100Hz, 1s) and LTD (52% decrease; p<0.001; Figure 13D) after low frequency stimulation (1Hz 15min) in *Bhlhe40* KO hippocampal slices compared to controls. There was no effect on paired pulse facilitation (Figure 13B), indicating the changes in plasticity are likely due to post-synaptic effects. However, we observed a greater response to current in the excitatory post synaptic potential (EPSP) slope, indicating a greater intrinsic response to stimulation (Figure 13A). Combined, this indicates a decrease in long term synaptic plasticity due to post-synaptic mechanisms. Notably, changes in synaptic plasticity are in response to a stimulation protocol, which are thought to induce transcriptional changes, which are likely directly or indirectly altered by deletion of *Bhlhe40*. That is, changes in gene expression as a result of *ex-vivo* stimulation have not been elucidated in this mouse model, however, IDE may be playing a role. By comparison, there is no stimulation protocol for measuring basal excitability. Therefore, changes in basal excitability are likely due to changes in the basal transcriptional profile as a result of *Bhlhe40* gene deletion, whereas changes in synaptic plasticity may be due to impaired transcriptional responses to *ex vivo* stimulation protocols.

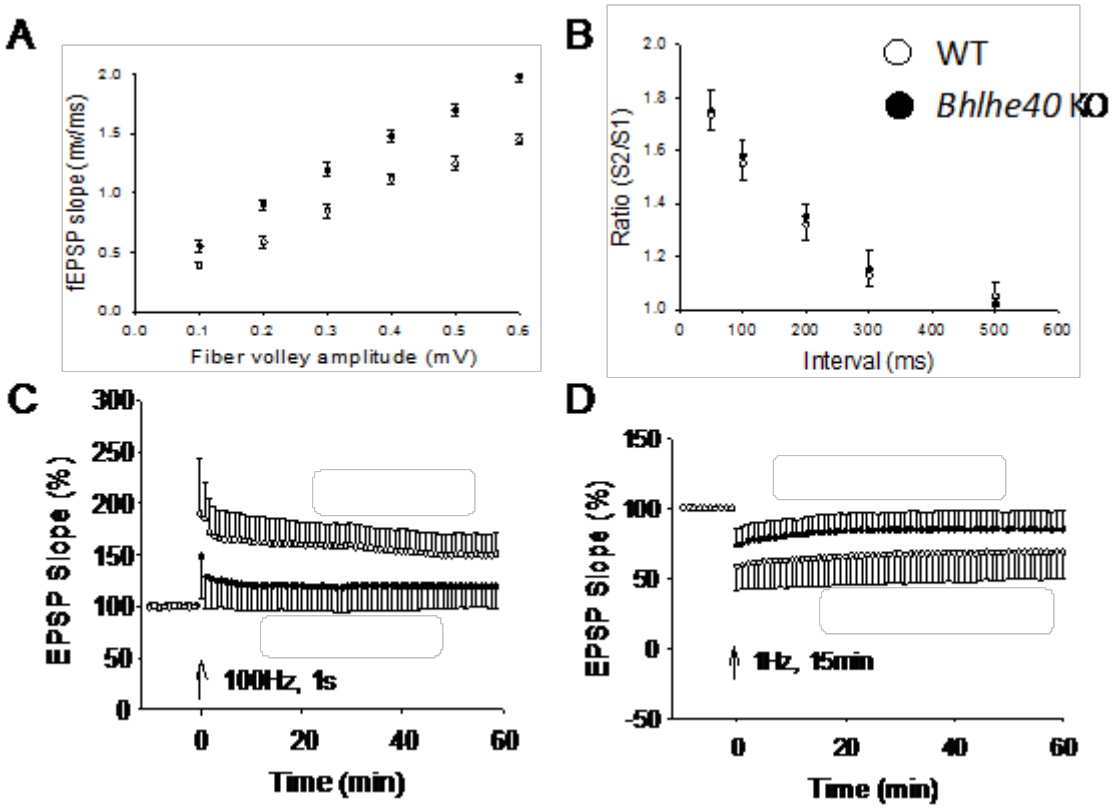

Figure 13. *Bhlhe40* KO mice have reduced hippocampal synaptic plasticity.
A) EPSP slope input/output curves were significantly different ($p<0.05$ by Shapiro Wilk normality test; $p<0.001$ by Mann-Whitney Rank Sum Test; n=9). B) Paired pulse facilitation not significantly impaired ($p=0.063$; n=5). C) There was a 60% reduction in LTP measured by EPSP slope 1hr following 1s of 100Hz stimulation (*Bhlhe40* KO: 120 +/- 20.7, WT: 150.5 +/- 21; $p<0.001$; n=5). D) There was a 52% reduction in LTD measured by EPSP slope 1hr following 15min of 1Hz stimulation (*Bhlhe40* KO: 85 +/- 12.8, WT: 68.5 +/- 19.5; $p<0.001$; n=5). Error bars are standard error of the mean.

Bhlhe40 KO mice do not have more-severe seizures

Given the fact hyperexcitability is a feature of epileptiform activity and that *Bhlhe40* KO on a mixed background showed increased KA-induced seizures (Jiang et al.,

2008), we investigated whether the same held true for congenic *Bhlhe40* KO mice. We induced behavioral seizures via intra-hippocampal KA infusion in six WT and six *Bhlhe40* KO 5-month old mice. Animals were monitored for six hours following an infusion of 227ng KA to dorsal hippocampus and assessed according to a seizure scale. There were no significant differences in latency to seizure initiation (Figure 14A), time seizing (Figure 14B), time from last seizure to end of the 6-hour monitoring period (Figure 14C), or maximum seizure score (Figure 14D).

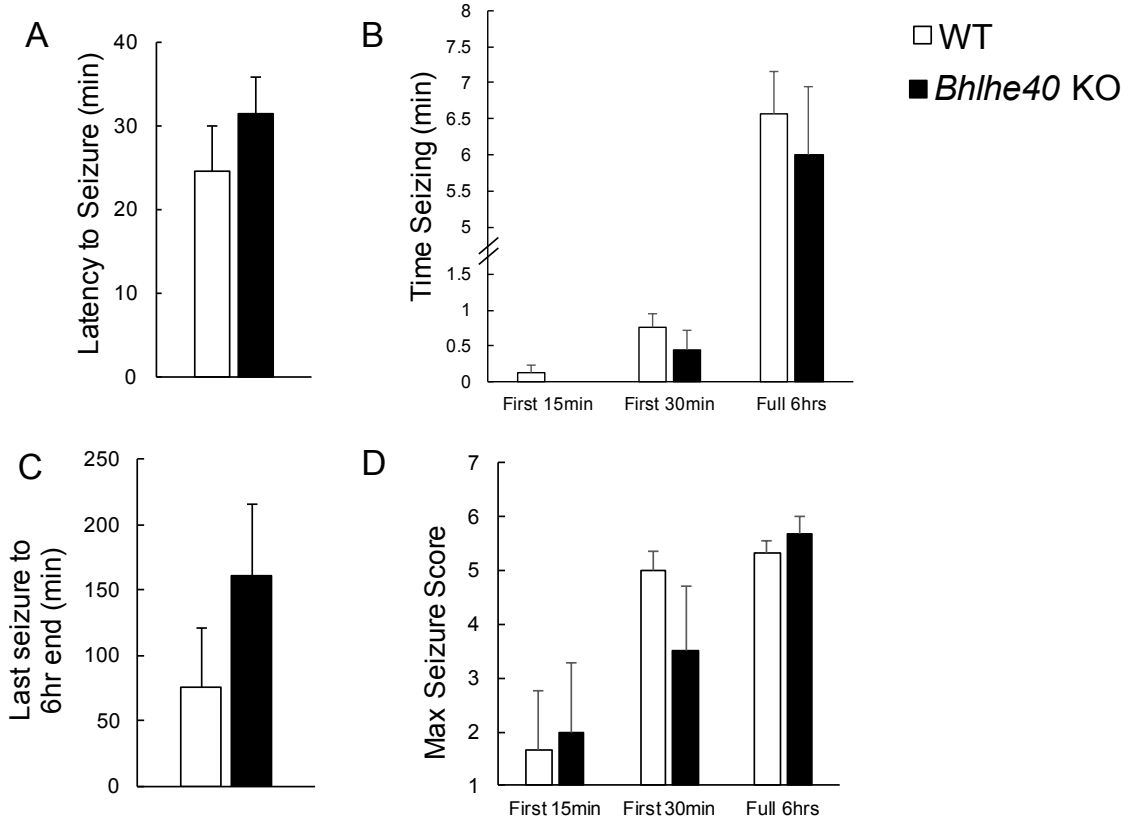

Figure 14. *Bhlhe40* KO mice do not have more-severe behavioral seizures.
Animals were infused with 227ngs of KA and monitored for six hours. A) Latency from infusion to first seizure, unpaired t-test $p>0.05$; B) Total time seizing over the first 15minutes, first 30 minutes, and full 6 hours, unpaired t-test $p>0.05$; C) Latency from last seizure to the end of the

six-hour monitoring period, unpaired t-test for each p>0.05; D) Seizure scale for maximum seizure response for the first 15 minutes, first 30 minutes, and full 6 hours, unpaired t-test for each p>0.05. N=6 for WT mice and n=5 for *Bhlhe40* KO mice (B,C), n=6 for *Bhlhe40* KO mice (A,D; including an animal that died during the monitoring period). Error bars are standard error of the mean.

Formalin fixed brain sections from *Bhlhe40* KO mice were stained with 1% cresyl violet acetate and measured for cell death in hippocampal area CA3. We accessed the intensity of the stain to the CA3 stratum pyramidale neuronal layer relative to CA3 stratum radiation (Figure 15, left), and the thickness (Figure 15, right) of the cell body layer to determine cell loss and apoptotic swelling, respectively.

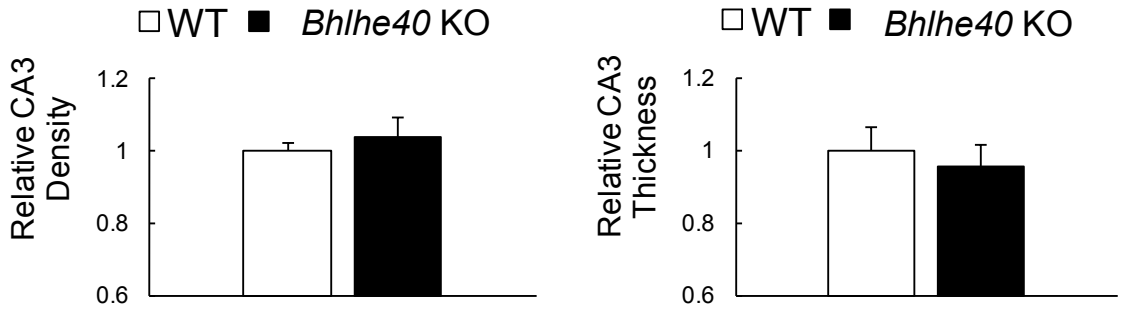

Figure 15. *Bhlhe40* KO mice do not have more cell death following KA infusion.
Neuronal death was quantified using Fiji software to measure integrated density of staining of the CA3 pyramidal neuron cell body layer relative to background staining (A; n=4; unpaired t-test p>0.05). Thickness of the CA3 cell body was assessed using Fiji software by measuring the length across the CA3 cell body layer to measure neuronal apoptotic swelling (B; n=4; unpaired t-test p>0.05).

Next, to further investigate the question of seizure susceptibility we looked at epileptiform activity on EEG before and after delivery of a low dose (57 ng) of KA.

Here, a lower drug concentration was used to prevent saturation EEG activity and to make possible differences in epileptiform activity visible. There were no differences in epileptiform activity following a saline infusion (Figure 16B). No animal had behavioral seizures following saline infusion and every animal had behavioral seizures following KA infusion. EEGs were evaluated for seizure severity (Figure 16C, D). EEG analysis was performed during the first 6 hours and the first 24-hour period following KA infusion. There was no significant difference in EEG activity between *Bhlhe40* KO and WT mice following KA infusion (repeated measures two-way ANOVA comparing genotype and time for each of three power bands; $p>0.05$ for each).

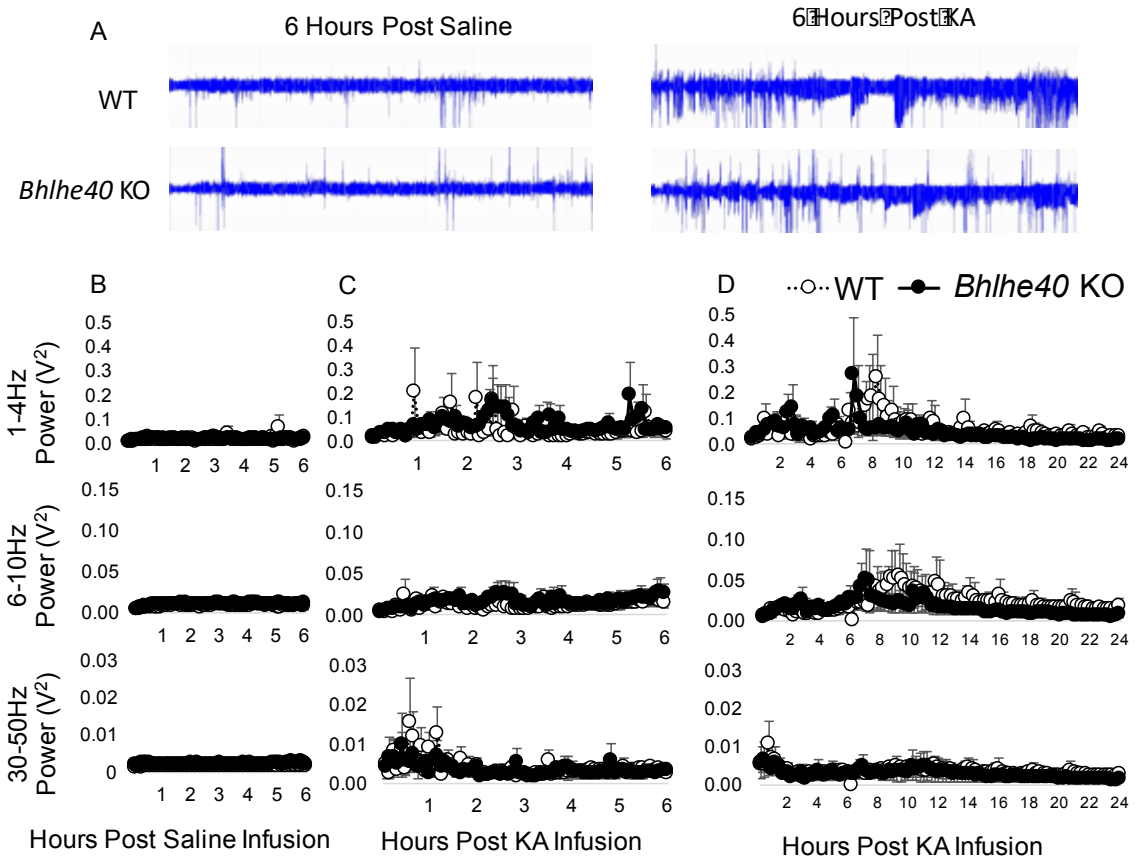

Figure 16. EEG responses to KA and saline infusion.
A) Example Traces of EEG activity six hours following saline and KA infusion in WT and *Bhlhe40* KO animals. The same animals are displayed for the saline and KA delivery for the WT and *Bhlhe40* KO examples. The Y axis for the EEG figures are +2mV to -2mV for each. EEG power over time for the first 6 hours at 5-minute intensity averages after B) saline, WT (n=6) and *Bhlhe40* KO (n=7) and C) KA, WT (n=6) and *Bhlhe40* KO (n=5; 2 outliers pulled). D) 15-minute intensity averages for 24 hours following KA infusion. B-D) 1-4 Hz activity is a surrogate for seizure scores 1-3, and 6-10Hz activity is a surrogate for seizure scores 4-6. 30-50Hz activity is known to precede seizure activity and is an additional ictal marker. Repeated measures two-way ANOVA was used for each dataset corresponding to figures B-D; $p>0.05$ for all. Error bars are standard error of the mean.

Bhlhe40 KO mice have increased anxiety

Behavior animals were run on an open field for 30 minutes to determine if there were any changes in exploration. Over the 30-minute period there were no changes in

time spent in the center or perimeter of the maze, nor in vertical rearing (Figure 17; left; two-way ANOVA = 0.063). However, *Bhlhe40* KO mice traveled less distance overall in the maze (Figure 17; right; unpaired t-test $p<0.05$). Distance traveled is an accepted measure for exploratory activity and thus indicates a possible increase in anxiety (Bailey and Crawley, 2009).

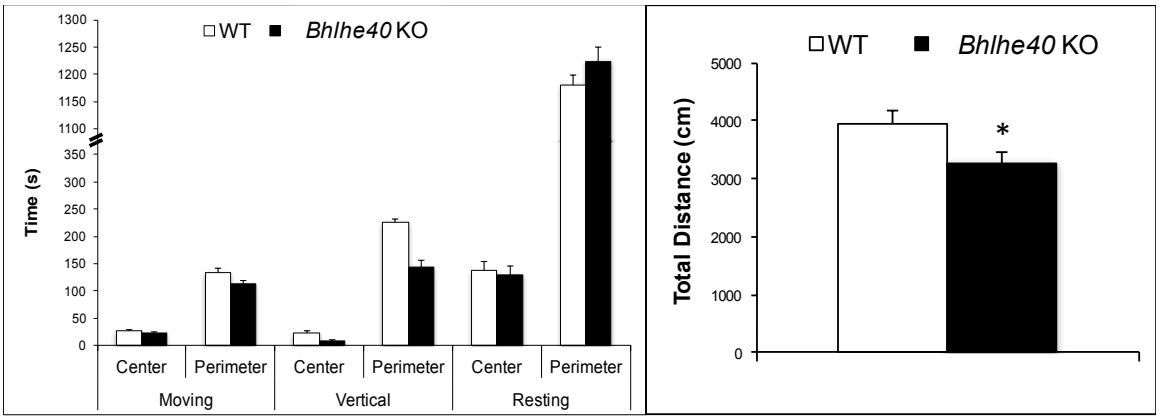

Figure 17. *Bhlhe40* KO mice have a decrease in exploratory activity.
Left: Time spent in each zone on the open field. Two-way ANOVA is not significant (p=0.063). Right: *Bhlhe40* KO mice traveled less overall distance on the open field (*=$p<0.05$). Error bars are standard error of the mean; n=12 WT and n=13 *Bhlhe40* KO.

Bhlhe40 KO mice do not have impaired learning and memory

We found no difference between *Bhlhe40* KO and WT mice on MWM performance. Specifically, performance was near identical on the initial MWM training and probes (Figure 18). There was, however, a trend toward impairments on MWM relearning on the reversal task (Figure 19). There was a trend on the reversal learning curve (p=0.067 by two-way ANOVA) as well as latency to the platform on the probe

trials (p=0.059 by two-way repeated ANOVA). In spite of these trends there was no effect on time spent in the goal quadrant on both the initial and reversal probe trails. There was also no effect on swim speed on either training.

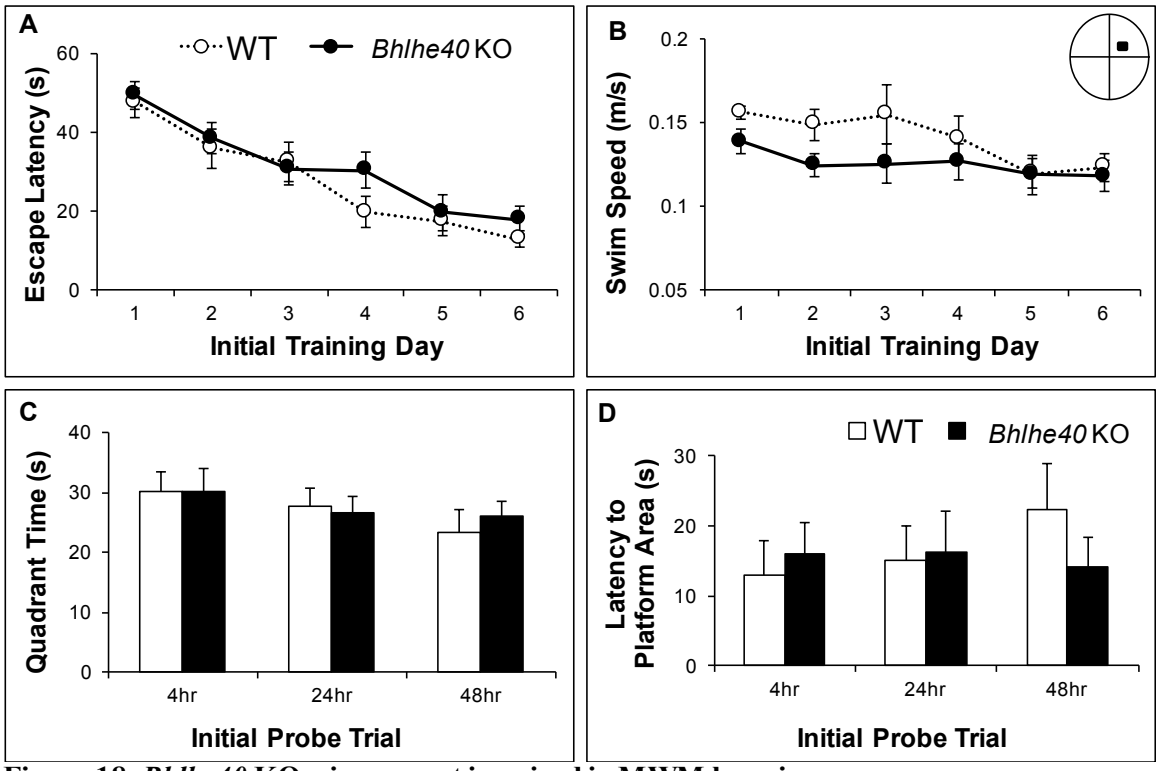

Figure 18. *Bhlhe40* KO mice are not impaired in MWM learning.
A) There was no change in escape latency nor swim speed (B) during training (did not pass repeated measures two-way ANOVA). C) There was also no change in platform recall as measured by time spent in the goal quadrant (upper right) and D) latency to the platform area. WT n=12, *Bhlhe40* KO n=13.

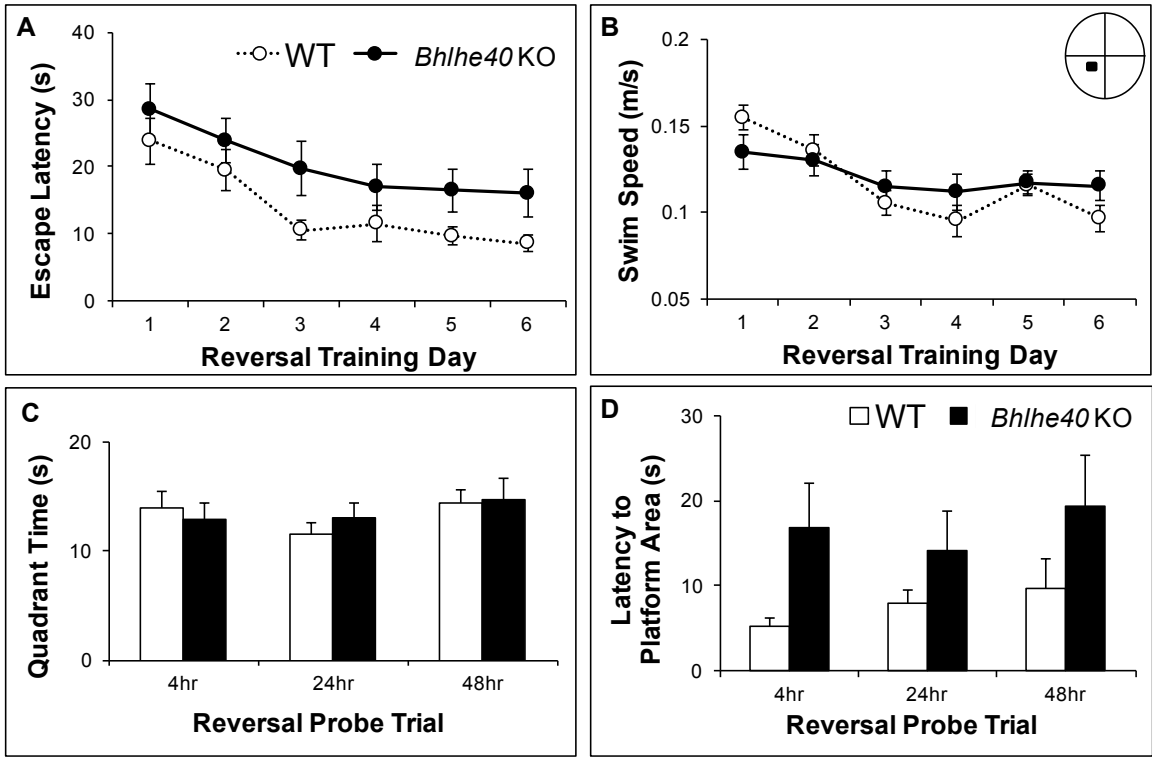

Figure 19. *Bhlhe40* KO mice do not have impaired MWM relearning
A) There is a nonsignificant trend in the reversal training escape latency (two-way repeated measures ANOVA p=0.067) with no effect on swim speed (B) during relearning. C)There was also an insignificant trend in the latency to the platform area in the probe trials (two-way repeated measures ANOVA p=0.059) with D) no effect on the quadrant times. WT n=12, *Bhlhe40* KO n=13.

Discussion

We found that *Bhlhe40* KO mice exhibit increases in excitability in CA1 neurons, but observed no change in seizure severity from intra-hippocampal KA injection, suggesting enhanced neuronal excitability in at least one component of the hippocampal circuit, but this was not sufficient to increase vulnerability seizures *in vivo*. Similarly, we found a decrease in synaptic plasticity at CA1 synapses in hippocampal slices from *Bhlhe40* KO mice, but saw no significant effect of Bhlhe40 deficiency on learning and

memory in the MWM. This suggests that deficits in long term synaptic plasticity at CA1 synapses do not necessarily predict deficits in learning and memory. Unexpectedly, we saw a decrease in exploratory activity of *Bhlhe40* KO mice in the open field test, which may be suggestive of increased anxiety and is in contrast to the reduction in anxiety seen in *Bhlhe40/Bhlhe41* double KO mice (Baier et al., 2014). This difference may suggest that Bhlhe41 supports a pro-anxiety phenotype and has an opposing role to Bhlhe40 in this regard.

An important finding of this research is the lack of enhanced seizure susceptibility in congenic *Bhlhe40* KO mice, particularly when compared to the *Bhlhe40* KO-mix mice (Jiang et al., 2008). It is possible that the changes in behavioral seizures are at least partly due to route of delivery since here we performed an intra-hippocampal delivery of KA, as opposed to the intraperitoneal injection used previously (Jiang et al., 2008). If this is the case, then the behavioral seizures reported previously could have been due to Bhlhe40-mediated mechanisms altering excitability in the amygdala or other non-hippocampal neuronal circuits. Possible anxiety changes by reduced exploration on open field may also support a role for Bhlhe40 in the amygdala. However, our group previously found that *Bhlhe40* KO-mix mice have a significant increase in LTD (Figure 21D; Appendix), as opposed to a reduction in LTD shown here in the congenic *Bhlhe40* KO mice. The change in LTD between mouse lines cannot be explained by changes in methodology, suggesting that there are at least some inherent differences between the strains.

We reason that the changes in seizure response and synaptic plasticity between congenic *Bhlhe40* KO and *Bhlhe40* KO-mix are most likely due to differences in the genes regulated by Bhlhe40 in the two different genetic backgrounds. Variation in the sequence of promoter regions or spacing of promoter elements in Bhlhe40 target genes between genetic backgrounds could alter Bhlhe40-mediated transcriptional regulation. For example, it is thought that Bhlhe40 represses p53 transcriptional activity by direct interaction, but only if the Bhlhe40 and p53 promoter elements are within a few bases of each other (Qian et al., 2012b). It was found previously that neuronal cell death paralleled seizure severity and that C57Bl/6 mice were more resistant to seizure-induced cell death than FVB mice or FVB and C57Bl/6 hybrids (Mohajeri et al., 2004). Together, this indicates that the change in genetic background to C57Bl/6 likely resulted in decreased seizure sensitivity to *Bhlhe40* gene deletion.

We were surprised to find that there was not an elevation in hippocampal insulin levels in *Bhlhe40* KO mice given the two-fold decrease in IDE protein levels. IDE, however, is known to have other substrates, including: Igf1 and Igf2; amylin; and Aβ, the protein that accumulates in the brains of Alzheimer's disease patients (Qiu et al., 2006). Notably, it was determined that double *Bhlhe40/Bhlhe41* KO mice have enhanced Igf2 signaling in cortex (Shahmoradi et al., 2015). Reductions in IDE levels may underlie the enhanced Igf2 signaling seen in these mice. Interestingly, the double *Bhlhe40/Bhlhe41* KO mice showed enhanced reversal learning on the MWM, which we did not observe in the *Bhlhe40* KO mice, suggesting that Bhlhe41 may play a role in learning and memory distinct from Bhlhe40. It is also interesting to note that *Bhlhe40* KO mice have decreased

body weight at age 5-6 months of age, an effect one would not predict if there were elevated insulin levels. In *Ide* knockout mice there was a three-fold elevation in serum insulin at all ages, but no change in body weight until 6 months of age when *Ide* knock out mice were significantly heavier than WT animals (Abdul-Hay et al., 2011). This suggests that 50% of normal IDE protein levels seen in *Bhlhe40* KO mice may be sufficient to maintain normal insulin homeostasis at baseline. This IDE reduction, however, may exacerbate Aβ pathology in Alzheimer's models, since IDE degrades Aβ and reduces Aβ-induced toxicity (Yin et al., 2012).

It was previously reported that Hes1 and Hey1, basic helix loop helix transcription factors related to Bhlhe40 (Sun et al., 2007a), transcriptionally repress *Ide* in the hippocampus following Notch activation (Leal et al., 2012). According to the Allen Brain Atlas, Hes1 and Hey1 are both expressed in hippocampal CA1 neurons, suggesting a possible relationship with Bhlhe40 transcriptional regulation. Bhlhe40 has been shown to be an inhibitor of Notch-mediated transcriptional activity in myoblasts (Sun et al., 2007b), suggesting that Bhlhe40 may be a negative regulator of notch-mediated repression of *Ide*. Additionally, we identified a possible Sp1 binding site in the *Ide* promoter, suggesting Bhlhe40 may transcriptionally upregulate *Ide* levels through direct DNA interaction. Further, hepatic Notch signaling positively correlates with insulin resistance (Valenti et al., 2013) and inhibition of Notch reduces insulin resistance (Pajvanti et al., 2012), thus demonstrating the interplay between Notch and insulin signaling. We propose a novel role for Bhlhe40 in regulating *Ide* expression, which has

significant implications for Alzheimer's disease pathology due to the role of IDE in degrading Aβ.

CHAPTER THREE: IMPLICATIONS AND FUTURE DIRECTIONS

In this dissertation I demonstrated that the transcription factor Bhlhe40 is involved in neuronal excitability and synaptic plasticity, although the mechanisms remain unknown. In spite of the insignificant change observed in hippocampal insulin levels, IDE is highly significantly downregulated in *Bhlhe40* KO mice. Additionally, IDE is known to have non-insulin substrates, including Igf2, which was reported elsewhere as elevated in cortex *Bhlhe40/Bhlhe41* double KO mice (Shahmoradi et al., 2015), corroborating the prediction of elevated IDE substrates. And because *Bhlhe40* gene expression is upregulated via insulin signaling (Yamada et al., 2003), it seems likely that Bhlhe40 would play a homeostatic role, acting to degrade insulin via IDE, which is still likely the case despite no significant difference in insulin levels observed in hippocampus of WT and *Bhlhe40* KO mice. This suggests that a 50% of normal IDE levels is not sufficient to reduce insulin levels at baseline. Nevertheless, it is conceivable that a reduction of IDE could affect the vulnerability of neurons to age-related neurodegenerative disorders and diabetes-related dysfunction and degeneration. Given that the tissue of focus for this research was the hippocampus, and not muscle, the prospects for Alzheimer's disease are interesting and merit further investigation.

Figure 20. Potential mechanism for Bhlhe40 in regulating *Ide* levels.

I identified a possible Sp1 binding site in the *Ide* gene promoter and given that *Ide* levels are decreased in *Bhlhe40* KO hippocampus and that Bhlhe40 can act as a transcriptional activator at Sp1 sites, it seems logical that Bhlhe40 may be acting at the *Ide* promoter via an Sp1 mediated binding interaction. As discussed in chapter one, this Sp1-mediated transcriptional activation would act like demonstrated here in Figure 20, however, this is speculative and needs to be validated in future research. I suggest that IDE substrates, starting with Igf2 be tested in the context of neuronal excitability and synaptic plasticity in future studies with these mice. Further, given the possible increase in anxiety shown here and a seizure effect reported previously on mixed background *Bhlhe40* KO mice (Jiang et al., 2008), but not via intra-hippocampal injections here, it suggests there may be an underlying role for Bhlhe40 in amygdala function. Fear learning may be impaired in these mice, for example. But perhaps most interestingly, would be to elucidate the regulatory network of *Ide* in the context of Alzheimer's disease. It is possible that Bhlhe40 and Hes1/Hey1 form a regulatory circuit to modulate *Ide* gene

expression, which may have important implications for understanding and treating Alzheimer's disease.

APPENDIX

Wrote Chapter: Kelly Hamilton, Yue Wang (Methods and Results)
Edited Chapter: Robert Lipsky
Collected Data: Yue Wang (National Institute on Aging)
Analyzed Data: Yue Wang
Citation: unpublished data

Abstract

Here we show that mice genetically null for the *Basic Helix Loop Helix Enhancer 40 Transcription Factor (Bhlhe40)* on a mixed genetic background (*Bhlhe40* KO-mix) have altered synaptic plasticity. Specifically, hippocampal slices from *Bhlhe40* KO-mix mice have reduced long term potentiation (LTP), and enhanced long term depression (LTD), and have an altered NMDA:AMPA ratio. Previously these mice were shown to have more-severe seizures than littermate wild-type controls (WT). These results suggest *Bhlhe40* KO-mix mice may exhibit enhanced seizure activity due to changes in post-synaptic glutamate receptors, which may be a core mechanism behind changes in synaptic plasticity shown here, and changes in behavioral seizures reported previously.

Introduction

The transcription factor Basic helix loop helix enhancer 40 (Bhlhe40) is involved in a number of pathways, most notably for its roles in circadian regulation, immune

function, and cancer (Sun et al., 2007a, Yamada and Miyamoto 2005, Davis and Turner 2001, Kato et al., 2014, Ow et al., 2014). Bhlhe40 has been most studied as a transcriptional repressor by binding to E-box sites in genomic promoter regions, however, Bhlhe40 can also act as a transcriptional activator by binding to Sp1 sites (Kato et al., 2014). Bhlhe40 can transcriptionally repress genes by binding to class B E-boxes as a homodimer (CACGTG; St-Pierre et al., 2002) or as a heterodimer with Bhlhe41, the sister protein to Bhlhe40 (Kato et al., 2014). Additionally, Bhlhe40 can interact with other basic helix loop helix transcription factors, e.g. MyoD, and other proteins to indirectly regulate gene expression (Ow et al., 2014).

In 2008, Jiang and colleagues identified a Bhlhe40 E-box binding site (CTCGTG) at promoter 4 for the *Brain derived neurotrophic factor (Bdnf)* gene and subsequently generated the *Bhlhe40* KO-mix mouse strain to investigate the role of *Bhlhe40* gene deletion on *Bdnf* gene expression in the hippocampus. Transcripts starting from the fourth exon of *Bdnf* (*Bdnf-4*) are activity dependent and play a role in synaptic plasticity and learning and memory (Jiang et al., 2008). As expected, the Jiang et al. team saw a de-repression of *BDNF-4* transcripts relative to the full length transcripts of BDNF, however, unexpectedly, they also noticed some of the animals had spontaneous seizures. To investigate the role of Bhlhe40 on seizure susceptibility they intraperitoneally (IP) injected mice with Kainic Acid (KA), the specific agonist for Kainate-type glutamate receptors and a known convulsant. They saw a marked increase in behavioral seizures in *Bhlhe40* KO-mix mice as measured by a seizure scale. It is known that *Bhlhe40* is expressed in the hippocampus (CA1 and subiculum) and in cortex layer 5 and that

Bhlhe40 gene expression increases in wild type rodents following IP injection (Rossner et al., 1997).

The model, proposed by the Jiang et al. (2008) study, was that Bhlhe40 was necessary to regulate activity-dependent BDNF, an excess of which could lead to hyperexcitability, supporting the BDNF hypothesis for epilepsy (Binder et al., 2001). Here, we investigated the electrophysiological properties of *Bhlhe40* KO-mix hippocampal slices.

Methods

Mice

Three to four months old male *Bhlhe40* KO-mix mice and WT mice were used in this study. *Bhlhe40* KO-mix mice were generated previously as described by Jiang et al. (2008).

Slice Preparation and Electrophysiology

Hippocampal slices were prepared as previously described (Wang et al. 2009). Briefly, transverse slices of whole brain were cut at 350 μm thick then allowed to recover for at least 1hr in room temperature artificial cerebral spinal fluid (ACSF), bubbled with 95/5% (O_2/CO_2). Field potentials were evoked by Schaffer Collateral (SC) stimulation and recorded in hippocampal area CA1 stratum radiatum using pulled borosilicate (1-3 MΩ) filled with ACSF. Pulses (30 μs duration at 0.033 Hz) were delivered through fine bipolar tungsten electrodes. The stimulation intensity used was approximately 30% of the maximum excitatory postsynaptic potential (EPSP). LTP was induced by high frequency stimulation (HFS; 100Hz, 1s) and LTD was induced by low frequency

stimulation (LFS; 1Hz, 15min). ACSF for LTP and LTD studies contained 50 μM picrotoxin to block $GABA_A$-mediated inhibitory action. Only slices with a steep input-output curve were used for recording. Slices were maintained at 30-32˚C during recording.

Whole-cell excitatory postsynaptic currents (EPSCs) were recorded from CA1 pyramidal neurons (Zhang et al. 2011). The neurons were visualized by differential interference contrast microscopy using a 40X water immersion lens. Series resistance was 6-10 MΩ. The patch electrode (3-5 MΩ) contained (in mM): 125 $CsMeSO_3$; 2.5 CsCl; 0.2 EGTA, 7.7 TEA; 20 HEPES; 8 NaCl, 4 Mg-ATP; 0.3 Na-GTP; 5 QX-314; pH 7.2; the osmolality was 280-290 mmol/kg. Series voltage steps (20 mV and 150 ms) from –70 mV to +40 mV generated AMPA and NMDAR currents simultaneously (Stellwagen and Malenka, 2006). To avoid capacitance transients generated by the step effect on the current, there was a delay of 50ms between the start of a step and pre-synaptic stimulation. Specific inhibitors of NMDA receptors (AP-5) and AMPA receptors (NBQX) were used. Data was collected using an Axopatch 200B (Molecular Devices, Sunnyvale, CA) amplifier. Signals were filtered at 2kHz, digitized at 10kHz, and analyzed using pCLAMP 8 software (Molecular Devices). Data was presented as the mean ± SEM and statistical comparisons were made using non-paired t-tests and Mann-Whitney Rank Sum Test.

Results

Basal synaptic transmission and cell excitability were significantly greater in *Bhlhe40* KO-mix mice. The input/output (I/O) curves of field EPSPs in slices from

Bhlhe40 KO-mix mice were much steeper compared to controls (Figure 21A). Paired-pulse facilitation (PPF; Figure 21B) was unaffected by *Bhlhe40* gene deletion. With inter-pulse intervals of 50, 100, 200, 300 and 500ms, the values for slices from KO mice were 1.78 ± 0.06, 1.55 ± 0.05, 1.35 ± 0.06, 1.12 ± 0.06 and 1.05 ± 0.05, respectively. The values for WT mice were 1.75 ± 0.06, 1.59 ± 0.05, 1.28 ± 0.07, and 1.1 ± 0.05, respectively ($n = 6$ and 8 slices from 5 pairs of mice, $p > 0.05$; paired t test).

We observed a significant decrease in LTP and a significant enhancement of LTD in slices from *Bhlhe40* KO-mix mice compared to controls. The values for LTP magnitudes were 188 ± 13.1% and 74 ± 18.4% of the normalized EPSP slope for WT slices and *Bhlhe40* KO-mix mice, respectively ($p<0.001$, paired t test). LTD was enhanced in hippocampal slices from *Bhlhe40* KO-mix mice (38 ± 18.4%) compared to WT (69 ± 16.2%; $p<0.01$).

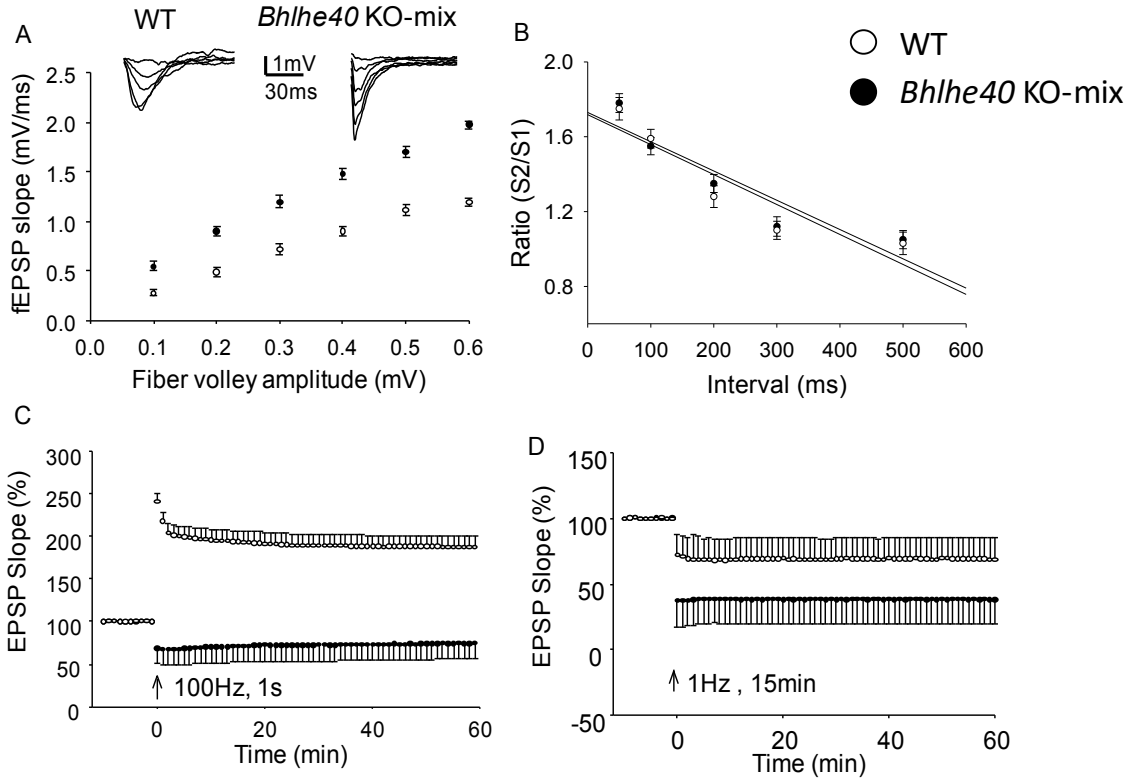

Figure 21. *Bhlhe40* KO-mix mice have altered hippocampal synaptic plasticity.
A) Amplitude of the fiber volley was plotted against the initial slope of the evoked EPSP. The input/output curves for WT and *Bhlhe40* KO-mix were significantly different, indicating that Bhlhe40 plays a role in basal synaptic transmission. B) PPF is normal in *Bhlhe40* KO-mix mice. The PPF curves were generated at inter-pulse intervals of 50, 100, 200, 300 and 500ms. C) LTP was significantly reduced in *Bhlhe40* KO-mix mice ($p<0.001$). LTP is induced by high frequency stimulation (100 Hz, 1 sec), with stimulation intensity that evoked about 30% of the maximum of EPSP. The plots were normalized initial slope of the EPSPs; each data point represents the averaged values for 1 min (three consecutive sweeping with an interval of 20 sec). Values are mean ± standard error of the mean (*Bhlhe40* KO-mix, 8 slices from 5 mice; WT, 8 slices from 6 mice). D) LTD was significantly enhanced in *Bhlhe40* KO-mix slices ($p<0.01$).

In slices from *Bhlhe40* KO-mix mice, both the NMDAR and AMPAR components of EPSCs were altered. The NMDA currents were reduced by 34%, compared to WT, 208.5 ± 12.8 pA vs. 228 ± 11.5 pA, at + 40mV (91%)171; AMPAR currents were enhanced by 16% in *Bhlhe40* KO-mix compared to the WT, 195 ± 12.8 pA vs. 171% ± 11.68 pA, n=10 from 8 mice in *Bhlhe40* KO-mix, and n = 10 from 6 mice for

WT). AMPAR-to-NMDAR current ratio was significantly increased 116.8% ± 10.3 compared to WT ($p < 0.05$; Figure 22).

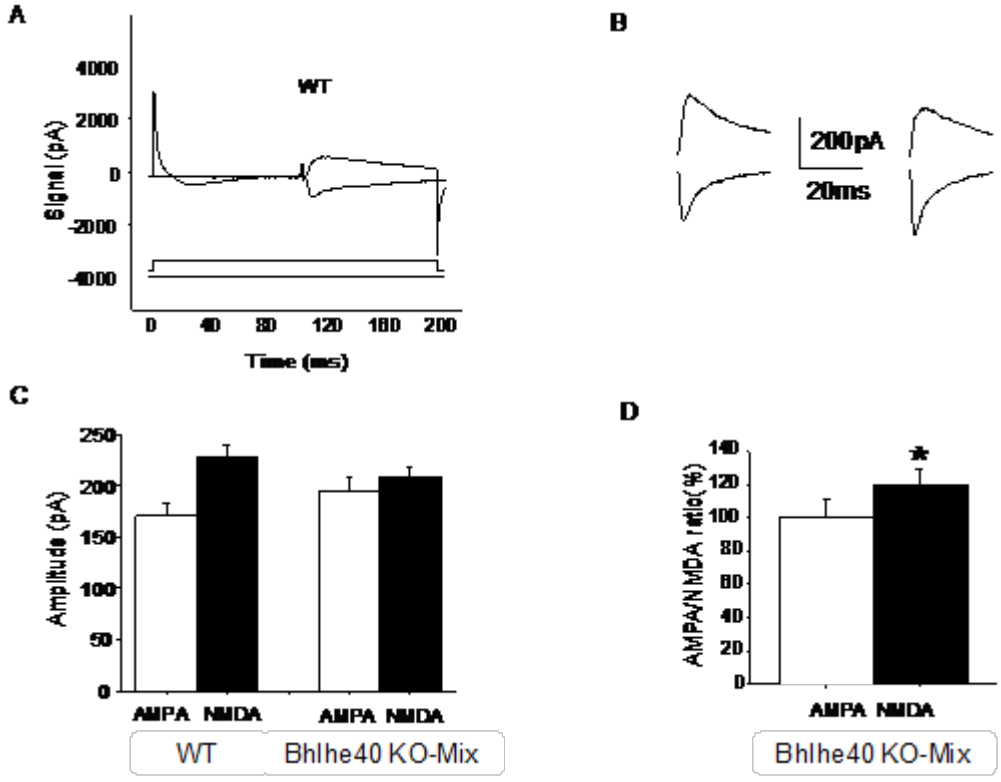

Figure 22. *Bhlhe40* KO-mix mice have increased NMDA:AMPA ratio.
A) Representative recording of NMDA and AMPA currents, from slice of WT mice. B) NMDAR/AMPAR Currents from WT and KO. The currents are recorded at +40mV or -70 mV, while cell held at -70 mV. C) Summary data for peak NMDAR and AMPAR currents amplitude, in WT or *Bhlhe40* KO-mix. D) Summary data for peak of the ratio of AMPAR-to-NMDAR currents, in WT or *Bhlhe40* KO-mix, there is a significant increase in *Bhlhe40* KO-mix mice ($p<0.05$).

Discussion

These results indicate *Bhlhe40* KO-mix mice have altered synaptic plasticity as well as changes in the AMPAR to NMDAR ratio. We propose that changes in AMPAR and NMDAR levels may be responsible for changes in hippocampal plasticity, reported here, and in behavioral seizure responses reported previously (Jiang et al., 2008). Further investigation is necessary to elucidate what changes in hippocampal gene expression are present in *Bhlhe40* KO-mix mice. We speculate that Bhlhe40 may transcriptionally repress ion channels in these mice, as well as *BDNF-4*, thereby acting to regulate homeostatic plasticity and neuronal excitability.

REFERENCES

Abdul-Hay SO, Kang D, McBride M, Li L, Zhao J, Leissring MA. (2011). Deletion of insulin-degrading enzyme elicits antipodal, age-dependent effects on glucose and insulin tolderance. *PLoS ONE*. 6(6): e20818. doi:10.1371/journal.prone.0020818.

Abdullah JM, Islam MR. (2012). Telemetric EEG and the Rat: A guide for neuroscientists. *Malays J Med Sci.* 19(4): 1-5.

Baier PC, Brzozka MM, Shahmoradi A, Reinecke L, Kroos C, et al. (2014) Mice Lacking the Circadian Modulators SHARP1 and SHARP2 Display Altered Sleep and Mixed State Endophenotypes of Psychiatric Disorders. PLoS ONE 9(10): e110310. doi:10.1371/journal.pone.0110310

Bailey KR, Crawley JN. (2009). Anxiety-related behaviors in mice. *Methods of Behavior Analysis in Neuroscience. 2nd Edition.* PMID: 21204329.

Barco A, Marie H. (2011). Genetic approaches to investigate the role of CREB in neuronal plasticity and memory. *Mol Neurobiol*. 44:330-349.

Belzung C, Turiault M, Griebel G (2014). Optogenetics to study the circuits of fear- and depression-like behaviors: A critical analysis. *Pharmacology, Biochemistry and Behavior* 122: 144-157.

Binder DK, Croll SD, Gall CM, Scharfman HE. (2001). BDNF and epilepsy: too much of a good thing? *Trends in Neurosciences.* 24(1): 47-53.

Boudjelal M, Taneja R, Matsaubara S, Bouillet P, Dolle P, Chambon P. (1997). Overexpression of Stra13, a novel retinoic acid-inducible gene of the basic helix-loop-helix family, inhibits mesodermal and promotes neuronal differentiation of P19 cells. *Genes Dev*. 11(16): 2052-2065.

Chen, J, Pan H, Lipsky RH, Perez-Gomez A, Cabrera-Garcia D, Fernandez-Sanchez MT, Novelli A, Marini AM. (2011). Cellular and molecular responses of cultured neurons to stressful stimuli. *Dose Response*. 9: 416-433.

Cheng A, Wan R, Yang J-L, Kamimura N, Son TG, Ouyang X, Luo Y, Okun E, Mattson MP. (2012). Involvement of PGC-1α in the formation and maintenance of neuronal dendritic spines. *Nat Commun*. 3: 1250.

Davis RL, Turner DL. (2001). Vertebrate hairy and enhancer of split related proteins: transcriptional repressors regulating cellular differentiation and embryonic patterning. *Oncogene*. 20: 8342-8357.

El-Hayek YF, Wu C, Zhang L. (2011). Early suppression of intracranial EEG signals predicts ischemic outcome in adult mice following hypoxia-ischemia. *Experimental Neurology*. 231:295-303.

Fisahn A. (2005). Kainate receptors and rhythmic activity in neuronal networks. *J Physiol*. 562(1): 65-72

Fortin A, Diez E, Rochefort D, Laroche L, Malo D, Rouleau GA, Gros P, Skamene E. (2001). Recombinant congenic strains derived from A/J and C57BL/6J: A tool for genetic dissection of complex traits. *Genomics*. 74: 21-35.

Guialtiere F, Marinelli C, Longo D, Pugnaghi M, Nichelli PF, Meletti S, Biagini G. (2013). Hypoxia markers are expressed in interneurons exposed to recurrent seizures. *Neuromol Med*. 15: 133-146.

Heinrich C, Nitta N, Flubacher A, Muller M, Fahrner A, Kirsch M, Freiman T, Suzuki F, Depaulis A, Frotscher M, Haas CA. (2006). Reelin deficiency and displacement of mature neurons, but not neurogenesis, underlie the formation of granule cell dispersion in the epileptic hippocampus. *J Neurosci.* 26(17): 4701-4713.

Hsiao SP, Huang KM, Chang HY, Chen SL. (2009). P/CAF rescues the Bhlhe40-mediated repression of MyoD transactivation. *Biochem. J*. 422: 343-352.

Hsiao SP, Chen SL. (2010). Myogenic regulatory factors regulate M-cadherin expression by targeting its proximal promoter elements. *Biochem J.* 428: 223-233.

Ivanova AV, Ivanov SV, Danilkovitch-Miagkova A, Lerman, MI. (2001). Regulation of Stra13 by the von Hippel-Lindau tumor suppressor protein, hypoxia, and the UBC9/ubiquitin proteasome degradation pathway. *The Journal of Biological Chemistry*. 276(18): 15306-15315.

Iizuka K, Horikawa Y. (2008). Regulation of lipogenesis via BHLHB2/DEC1 and ChREBP feedback looping. *Biochemical and Biophysical Research Communications*. 374: 95-100.

Jiang X, Tian F, Du Y, Copeland NG, Jenkins NA, Tessarollo L, Wu X, Pan H, Hu XZ, Xu K, Kenney H, Egan SE, Turley H, Harris AL, Marini AM, Lipsky RH. (2008). BHLHB2 controls Bdnf promoter 4 activity and neuronal excitability. *J Neurosci* 28:1118-1130.

Jin Z, Jin Y, Kumar-Mendu S, Degerman E, Groop L, Binir B. (2011). Unsulin reduces neuronal excitability by turning on GABA(A) channels that generate tonic current. *PLoS ONE*. 6(1): e16188.

Kato Y, Kawamoto T, Fujimoto K, Noshiro M (2014). Dec1/Stra13/Sharp2 and Dec2/Sharp1 coordinate physiological processes, including circadian rhythms in response to environmental stimuli. *Current Topics in Developmental Biology*. Vol 110 (10): 339-372.

Kim J, D'Annibale S, Magliozzi R, Low TY, Jansen P, Shaltiel IA, Mohammed S, Heck AJR, Medema RH, Guardavaccaro D. (2014). USP17- and $SCF^{\beta TrCP}$ –regulated degradation of DEC1 controls the DNA damage response. *Mol. Cell. Bio. (Epub ahead of print)*. doi: 10.1128/MCB.00530-14.

Leal M, Surace EI, Holgado MP, Farrari CC, Tarelli R, Pitossi F, Wisniewski T, Castano EM, Morelli L. (2012). Notch signaling proteins HES-1 and Hey-1 bind to insulin degrading enzyme (IDE) proximal promoter and repress its transcription and activity: Implications for cellular Aβ metabolism. *Biochemica et Biophysica Acta*. 1823: 227-235.

Levesque M, Avoli M. (2013). The kainic acid model of temporal lobe epilepsy. *Neurosci Biobehav Rev*. 37(10 Pt 2): 2887-2899.

Li Y, Xie M, Yang J, Deng R, Wan Y, Yan B. (2006). The expression of antiapoptotic protein survivin is transcriptionally upregulated by Dec1 primarily through multiple sp1 binding sites in the proximal promoter. *Oncogene*. 25: 3296-3306.

Liu H, Cao Y, Basbaum AI, Mazarati AM, Sankar R, Wasterlain CG. (1999). Resistance to excitotoxin-induced seizures and neuronal death in mice lacking the preprotachykinin A gene. *PNAS*. 96 (21): 12096-12101.

Long Q, Fun C, Kai W, Luo Q, Xin W, Wang P, Wang A, Wang Z, Han R, Fei Z, Qiu B, Liu W. (2014). Hypoxia inducible factor-1α expression is associated with hippocampal apoptosis during epileptogenesis. *Brain Research*. 1590: 20-30.

Lutas A, Yellen G. (2013). The ketogenic diet: metabolic influences on brain excitability and epilepsy. *Trends in Neurosciences*. 36(1): 32-40.

Mathis DM, Furman JL, Norris CM (2011). Preparation of acute hippocampal slices from rats and transgenic mice for the study of synaptic alterations during aging and amyloid pathology. *J. Vis. Exp*. (49), e2330, doi:10.3791/2330.

Middei S, Ammassari-Teule M, Marie H. (2014). Synaptic plasticity under learning challenge. *Neurobiology of Learning and Memory*. 115: 108-115.

Mohajeri MH, Madani R, Saini K, Lipp H-P, Nitsch RM, Wolfer DP. (2004). The impact of genetic background on neurodegeneration and behavior in seizured mice. *Genes, Brain, and Behavior*. 3: 228-239.

Nagata T, Takahashi Y, Sugahara M, Murata A, Nishida Y, Ishikawa K, Asai S. (2004). Profiling of genes associated with transcriptional responses in mouse hippocampus after transient forebrain ischemia using high-density oligonucleotide DNA array. *Molecular Brain Research*. 121: 1-11.

O'Niel HC, Lavarty DC, Patzlaff NE, Cohen BN, Fonck C, McKinney S, McIntosh JM, Lindstrom JM, Lester HA, Grady SR, Marks MJ. (2013). Mice expressing the

ADNFLE valine 287 leucine mutation of the B2 nicotinic acetylcholine receptor subunit display increased sensitivity to acute nicotine administration and altered presynaptic nicotinic receptor function. *Pharmacology, Biochemistry and Behavior* 103: 603-621.

Ow JR, Tan YH, Jin Y, Bahirvani AG, Taneja R. (2014). Stra13 and Sharp-1, the non-grouchy regulators of development and disease. *Current Topics in Developmental Biology*. Vol 110 (9): 317-338.

Pajvani UB Shawber CJ, Samuel VT, Birkenfeld AL, Shulman GI, Kitajewski J, Accili D. (2012). Inhibition of Notch signaling ameliorates insulin resistance in a FoxO1-dependent manner. *Nature Medicine*. 17(8): 961-967.

Puttachary S, Sharma S, Stark S, Thippeswamy T. (2015). Seizure-induced oxidative stress in temporal lobe epilepsy. *BioMed Research International*. 745613.

Qian Y, Zhang J, Yan B, Chen X. (2008). DEC1, a basic helix-loop-helix transcription factor and a novel target gene of the p53 family, mediates p53-dependent premature senescence. *J. Biol. Chem*. 283: 2896-2905.

Qian Y, Jung Y-S, Chen X. (2011). ΔNp63, a target of DEC1 and histone deacetylase 2, modulates the efficacy of histone deacetylase inhibitors in growth suppression and keratinocyte differentiation. *Journal of Biological Chemistry*. 286(14): 12033-12041.

Qian Y, Jung Y-S, Chen X. (2012a). Differentiated embryo-chondrocyte expressed gene 1 regulates p53-dependent cell survival versus cell death through macrophage inhibitory cytokine-1. *PNAS*. 109(28): 11300-11305.

Qian Y, Jung Y-S, Chen X. (2012b). DEC1 and MIC-1: New players of p53-dependent cell fate decision. *Cell Cycle*. 11:19, 3525,3526.

Qian Y, Zhang J, Jung Y-S, Chen X. (2014). DEC1 coordinates with HDAC8 to differentially regulate Tap73 and ΔNp73 expression. *PLoS ONE*. 9(1): e84015.

Qiu W-E, Folstein MF. (2006). Insulin, insulin degrading enzyme and amyloido-β peptide in Alzheimer's disease: review and hypothesis. *Neurobiology of Aging*. 27: 190-198.

Rogner UC, Avner P. (2003). Congenic mice: Cutting tools for complex immune disorders. *Nature Review Immunology*. 3: 243-252.

Rossner MJ, Dorr J, Gass P, Schwab, MH, Nave K-A. (1997). SHARPs: Mammalian enhancer-of-split-and hairy-related proteins coupled to neuronal stimulation. *Molecular and Cellular Neurosci.* 9: 460-475.

Scharfman HE. (2005). Brain-derived neurotrophic factor and epilepsy – A missing link? *Epilepsy Currents*. 5(3): 83-88.

Seuter S, Pehkonen P, Heikkinen S, Carlberg C. (2013). The gene for the transcription factor Bhlhe40/Dec1/Stra13 is a dynamically regulated primary target of the vitamin D receptor. *Journal of Steroid Biochemistry and Molecular Biology*. 136: 62-67.

Shahmoradi A, Radyushkin K, Rossner MJ. (2015). Enhanced memory consolidation in mice lacking the circadian modulators Sharp1 and -2 caused by elevated Igf2 signaling in the cortex. *PNAS*. 112(27): E3582-9.

Shipton OA, Paulsen O. (2013). GluN2A and GluN2B subunit-containing NMDA receptors in hippocampal plasticity. *Phil. Trans. R. Soc. B.* 369: 20130163.

St-Pierre B, Flock G, Zacksenhaus E, Egan SE. (2002). Stra13 homodimers repress transcription through class B E-box elements. *Journal of Biological Chemistry.* 277(48): 46544-46551.

Stellwagen D, Malenka RC. (2006). Synaptic scaling mediated by glial TNF-alpha. *Nature*. 440: 1054-1059.

Shih H-M, Liu Z, Towle HC. (1995). Two CACGTG motifs with proper spacing dictate the carbohydrate regulation of hepatic gene transcription. *The Journal of Biological Chemistry*. 270(37): 21991-21997.

Sun H, Ghaffari S, Taneja R (2007a). BHLH-Orange transcription factors in development and cancer. *Translational Oncogenomics.* 2: 107-120.

Sun H, Li L, Cercherat C, Gulbagaci NT, Acharjee S, Li J, Chung T-K, Thin TH, Taneja R. (2007b). Stra13 regulates satellite cell activation by antagonizing Notch signaling. *The Journal of Cell Biology.* 177(4): 647-657.

Suzuki J. (2013). Neuronal mechanism of epileptogenesis in EL mouse. *Proc. Jpn. Acad., Ser. B.* 89: 270-280.

Valenti L, Mendoza RM, Rametta R, Maggioni M, Kitajewski, Shawber CJ, Pajvani. (2013). Hepatic notch signaling correlates with insulin resistance and nonalcoholoic fatty liver disease. 62: 4052-4062.

Wang Y, Greig N-H, Yu Q-S, Mattson M-P (2009) Presenilin-1 mutation impairs cholinergic modulation of synaptic plasticity and suppresses NMDA currents in hippocampus slices. *Neurobiol Aging*. 30:1061-1068.

Wang F Song YF, Yin J, Liu Z-H, Mo X-D, Wang D-G, Gao L-P, Jing Y-H. (2014). Spatial memory impairment is associated with hippocampal insulin signals in ovariectomized rats. *PLoS ONE*. 9(8): e104450. doi:10.1371/journal.prone.0104450.

Wong GT. (2002). Speed congenics: Applications for transgenic and knock-out mouse strains. *Neuropeptides*. 36(2-3): 230-236.

Yamada K, Kawata H, Shou Z, Mizutani T, Noguchi T, Miyamoto K. (2003). Insulin induces the expression of the Sharp-2/Stra13/Dec1 gene via a phosphoinositide 3-kinase pathway. *The Journal of Biological Chemistry*. 278(33): 30719-30724.

Yamada K, Ogata-Kawata H, Matsuura K, Miyamoto K. (2005). SHARP-2/Stra13/DEC1 as a potential repressor of phosphoenolpyruvate carboxykinase gene expression. *FEBS Letters*. 579: 1509-1514.

Yamada Z, Miyamoto K. (2005). Basic helix-loop-helix transcription factors, BHLHB2 and BHLHB3; their gene expressions are regulated by multiple extracellular stimuli. *Frontiers in Bioscience*. 10: 3151-3171.

Yin F, Zhang Y, Guo L, Kong S, Liu J. (2012). Geniposide regulates insulin-degrading enzyme expression to inhibit the cytotoxicity of Ab in cortical neurons. *CNS & Neurological Disorders – Drug Targets*. 11: 1045-1051.

Zhang J, Wang Y, Chi Z, Emily P, Bugayenko A, Wang H, Xiong Y, Mikhail V, Mattson MP, Dawson TM, Dawson VL (2011) Thorase, A Novel AAA+ ATPase, regulates AMPA receptor-dependent synaptic plasticity and behavior. *Cell* 145: 284-299.

BIOGRAPHY

Kelly Andrew Hamilton graduated from Hayfield High School, Alexandria, Virginia, in 2004. He received his Bachelor of Science in Psychology from George Mason University in 2008. He received his Doctorate of Philosophy in Neuroscience from George Mason University in 2016. He is an Eagle Scout and an amateur guitarist.